HHS Public Access

Author manuscript

Nat Struct Mol Biol. Author manuscript; available in PMC 2020 November 11.

Published in final edited form as:

Nat Struct Mol Biol. 2020 June ; 27(6): 550–560. doi:10.1038/s41594-020-0424-6.

Ubiquitin chain-elongating enzyme UBE2S activates the RING E3 ligase APC/C for substrate priming

Raquel C. Martinez-Chacin[1], **Tatyana Bodrug**[2], **Derek L. Bolhuis**[1], **Katarzyna M. Kedziora**[3], **Thomas Bonacci**[1], **Alban Ordureau**[4], **Morgan E. Gibbs**[5], **Florian Weissmann**[6], **Renping Qiao**[6], **Gavin D. Grant**[2], **Jeanette G. Cook**[1,2], **Jan-Michael Peters**[6], **J. Wade Harper**[4], **Michael J. Emanuele**[1,*], **Nicholas G. Brown**[1,*]

[1]Department of Pharmacology and Lineberger Comprehensive Cancer Center, University of North Carolina School of Medicine, Chapel Hill, NC 27599, USA

[2]Department of Biochemistry and Biophysics and Lineberger Comprehensive Cancer Center, University of North Carolina at Chapel Hill, Chapel Hill, North Carolina 27599, USA

[3]Department of Genetics, University of North Carolina at Chapel Hill, Chapel Hill, North Carolina 27599, USA

[4]Department of Cell Biology, Blavatnik Institute of Harvard Medical School, Boston, MA 02115, USA

[5]Department of Chemistry, University of North Carolina at Chapel Hill, Chapel Hill, North Carolina 27599, USA

[6]Research Institute of Molecular Pathology (IMP), Vienna Biocenter (VBC) Campus-Vienna-Biocenter 1, 1030 Vienna, Austria

Abstract

The interplay between E2 and E3 enzymes regulates the polyubiquitination of substrates in eukaryotes. Among the several RING-domain E3 ligases in humans, many utilize two distinct E2s for polyubiquitination. For example, the cell cycle regulatory E3, human Anaphase-Promoting Complex/Cyclosome (APC/C), relies on UBE2C to prime substrates with ubiquitin (Ub) and UBE2S to extend polyubiquitin chains. However, the potential coordination between these steps in

*Correspondence should be addressed to M.J.E. (emanuele@email.unc.edu) or N.G.B. (nbrown1@med.unc.edu).

AUTHOR CONTRIBUTIONS

RCMC, TB, KMK, TB, AO, MEG, JMP, JWH, MJE, NGB designed research supervised by JGC, JMP, JWH, MJE, and NGB; RCMC, TB, DLB, KMK, TB, AO, MEG, FW, RQ, and GDG performed research and/or contributed new reagents; RCMC, TB, KMK, TB, AO, MEG, JGC, JMP, JWH, MJE, and NGB analyzed data; and RCMC, TB, MJE, and NGB wrote the paper.

COMPETING INTERESTS

The authors declare no competing interests.

REPORTING SUMMARY

Further information on research design is available in the Reporting Summary linked to this article.

CODE AVAILABILITY

All codes utilized in this study are available from the authors upon request.

DATA AVAILABILITY

All data generated and analyzed in this study are available as Source Data.

ubiquitin chain formation remains undefined. While numerous studies have unveiled how RING E3s stimulate individual E2s for Ub transfer, here we change perspective to describe a case where the chain-elongating E2 UBE2S feeds back and directly stimulates the E3 APC/C to promote substrate priming and subsequent multiubiquitination by UBE2C. Our work reveals an unexpected paradigm for the mechanisms of RING E3-dependent ubiquitination and for the diverse and complex interrelationship between components of the ubiquitination cascade.

INTRODUCTION

The conjugation of ubiquitin (Ub) onto proteins is a key cellular process that mediates eukaryotic protein regulation. Polyubiquitination of targeted substrates (the linkage of several ubiquitins onto a single target) can induce changes to subcellular localization, alter protein function, or lead to proteasomal degradation, an important aspect of cell cycle control. In humans, E1, >30 E2s, and >600 E3 enzymes coordinate to polyubiquitinate proteins. The E1 mediates the transfer of Ub to the catalytic cysteine of an E2 to form an E2~Ub intermediate (~denotes covalent); an E3 mediates the transfer of Ub from the E2~Ub intermediate to a substrate. There are three major classes of E3s (RBRs, HECTs, and RINGs). The largest family of E3s contain a RING domain and serve as a scaffold to recruit both the E2~Ub and the substrate while simultaneously facilitating the transfer of Ub to substrate lysines (reviewed in[1,2]). As severe consequences result from the dysregulation of polyubiquitination, i.e. several cancers and developmental disorders, this process must be tightly controlled[3].

RING E3 ligases switch between active and inactive states through precise regulatory control that ensures specificity and timing of polyubiquitination events[4]. Activators, inhibitors, and post-translational modifications of RING E3s coordinate to control accurate cell cycle timing. Polyubiquitination leading to proteasomal degradation drives the cell cycle and is primarily mediated by the Cullin-RING ligase superfamily, which includes SKP1-CUL1-F-box proteins (SCFs) and the Anaphase-Promoting Complex/Cyclosome (APC/C)[5,6]. Both E3 subfamilies use multiple E2s for polyubiquitination. Through multiple rounds of E2 binding in a multi-step process and with cooperation between different E2s, these E3s facilitate the formation of Ub chains with multiple linkage types[7–9]. Yet, the details of how several E2s coordinate with a single E3 scaffold for polyubiquitination remain unclear. In our effort to dissect this process, we discovered the activating role of an E2 in E3 function in the context of the APC/C and its cognate E2s, UBE2C(UBCH10) and UBE2S.

The APC/C is a 1.2 MDa multi-subunit complex that polyubiquitinates key cell cycle regulators (e.g. cyclins and securin) to direct chromosomal segregation, cytokinesis, G1 maintenance, and multiple aspects of neurobiology (reviewed in[10–12]). The APC/C can be divided into two sub-complexes termed the “Arc lamp” and “Platform”. The Arc lamp provides structural reinforcement while the Platform contains the catalytic module where the cullin-like subunit APC2 and the RING domain subunit APC11 facilitate Ub transfer[13,14]. APC/C activity is regulated through coactivators, CDH1 and CDC20, and inhibitors, EMI1 and Mitotic Checkpoint Complex (MCC)[15–18]. The APC/C remains in an inactive conformation until a coactivator binds[19]. Coactivator binding plays two important roles.

First, coactivators recruit substrates to the APC/C. Second, they reposition the APC2–APC11 catalytic module from an inactive to an active state[19–23]. This mobilizes the catalytic module to expose the UBE2C-binding site and facilitates UBE2C activation for ubiquitination[19,24,25]. The WD40 domain of the scaffolding subunit APC1 (APC1^{WD40}) is critical for mediating this conformational change; deletion of APC1^{WD40} has been shown to lock the catalytic module in the downward position, blocking the binding site of UBE2C while leaving UBE2S binding unaffected[26].

Recent structural studies have shown that the APC/C uses distinct architectures to perform specific polyubiquitination steps with UBE2C and UBE2S (Fig. 1a, Extended Data Fig. 1)[24,25,27]. Upon coactivator binding, UBE2C~Ub is recruited and activated by APC2^{WHB}–APC11^{RING} to prime the substrate with its first Ub[19,24,25,28,29]. APC/C next catalyzes two types of reactions: multiubiquitination via UBE2C, with Ub transferred to additional substrate lysines or to the initial Ub, resulting in short chains; or alternatively, chain elongation via UBE2S, which forms K11-linked Ub chains (Fig 1a, bottom, Extended Data Fig. 1)[27,30–33]. During processive multiubiquitination, UBE2C~Ub is clamped by the APC2^{WHB}–APC11^{RING} in the vicinity of the RING surface (hereafter referred to as “exosite”) which binds a substrate-linked Ub to facilitate processive affinity amplification (PAA)[27,34]. For Ub chain elongation, the RING exosite positions the substrate-linked acceptor Ub to receive a Ub from UBE2S, extending the chain[27,32,33,35–37]. UBE2S~Ub binds to a distinct surface on APC2 via its ubiquitin-conjugating (UBC) domain and is uniquely tethered by its positively-charged C-terminal peptide to a groove formed by the APC2–APC4 interface[24,27,37,38]. Critically, the elongation step carried out by UBE2S requires a substrate that has already been primed with Ub by the UBE2C[27,31–33]. These enzymatic modalities allow for diverse Ub-topologies that subsequently tune substrate degradation efficiency, with branched chains increasing the protein degradation rate[39].

How are the regulatory states of E3s and the multiple E3–E2 architectures coordinated to ensure efficient substrate polyubiquitination? Here, we use biochemical and biophysical approaches coupled with mutagenesis and structural analysis to define a new mechanism for APC/C activation. We show that the binding of the “secondary” E2, UBE2S, to the APC2–APC4 groove accelerates the rate-limiting first ubiquitination step by APC/C-UBE2C. UBE2S utilizes a binding site distinct from the coactivators to stimulate the E3 APC/C to recruit and activate its counterpart E2 UBE2C. Our results demonstrate a new role for E2s in effecting E3 conformation and activity, thereby controlling E2-E3 cascades and substrate polyubiquitination. Finally, our work shows that a thorough understanding of the interrelationship between E3s and their corresponding E2s remains to be developed.

RESULTS

UBE2S Elongates Ub Chains on APC/C Substrates and Increases the Rate of Substrate Ubiquitination

The APC/C must alternate between different architectures for substrate polyubiquitination by its two E2s[27]. To investigate the interplay between UBE2S, the secondary E2 that elongates Ub chains, and UBE2C, the E2 that initiates polyubiquitination, we used our recombinant APC/C^{CDH1} system. We recapitulated ubiquitination reactions with APC/

C^{CDH1} and UBE2C, titrated UBE2S, and collected reactions at time points indicated (schematic in Fig. 1b). Modification of canonical APC/C substrates, the N-terminal fragment of cyclin B ($CycB^{NTD*}$) and Securin*, were monitored and quantified. As expected, the addition of UBE2S to APC/C^{CDH1}-UBE2C-mediated polyubiquitination reactions induced the formation of longer Ub chains on the substrates (Fig. 1b, Extended Data Fig. 2). Surprisingly, quantification of the fraction of remaining substrate over time revealed that UBE2S increased the substrate modification rate by 2-fold in comparison to UBE2C alone reactions (Fig. 1c, Extended Data Fig. 2, compare conditions 0 μM UBE2S with 5 μM UBE2S). As UBE2S cannot directly ubiquitinate substrates as an initiating E2, this suggests that the Ub chain elongating E2 UBE2S functions in undefined ways to influence the dynamics of substrate priming and/or multiubiquitination by APC/C^{CDH1}-UBE2C.

UBE2S C-terminal Peptide (CTP) Enhances Substrate Priming and Multiubiquitination by APC/C-UBE2C

Dynamic Ub chain elongation is facilitated by the multivalent binding of UBE2S to the APC/C[27,35,37]. To understand how UBE2S increases the rate of depletion of unmodified substrate by APC/C-UBE2C, we sought to determine if the catalytic activity of UBE2S or the binding of a UBE2S domain to APC/C is responsible for this effect. UBE2S contains a UBC domain (residues 1-156) that includes the catalytic cysteine, a linker (residues 157-203), and a C-terminal peptide (CTP, residues 204-222) that is crucial for UBE2S recruitment to the APC/C (Fig. 2a). Variants of UBE2S were added to APC/C^{CDH1}-UBE2C-dependent polyubiquitination reactions and the levels of unmodified $CycB^{NTD*}$ were quantified. While we observe an increase in substrate depletion when an active UBE2S UBC domain is added, this variant is deficient for Ub chain elongation in an APC/C-dependent manner (Extended Data Fig. 3a–c), suggesting that its effects are APC/C independent. Surprisingly, the addition of a catalytically inactive (C95K) UBE2S accelerated substrate depletion, indicating that UBE2S binding to the APC/C influences APC/C^{CDH1}-UBE2C activity (Extended Data Fig. 3a–b). Since the UBE2S UBC domain and the CTP are known to bind to distinct surfaces on the APC/C, we tested whether the catalytically dead (C95K) UBC domain or the $UBE2S^{CTP}$ alone could accelerate substrate depletion. We unexpectedly found that the non-enzymatic fragment $UBE2S^{CTP}$ is sufficient for increasing the rate of substrate depletion similar to full-length UBE2S (Fig. 2b, Extended Data Fig. 3d).

To characterize whether the effects of the $UBE2S^{CTP}$ are specific to APC/C-UBE2C-dependent priming or multiubiquitination, we undertook a comparison of two types of substrate: the unmodified substrates CycB* and Securin* which go through priming and multiubiquitination, and the Ub-linked substrates Ub-CycB* and Ub-Securin* which have a genetically-fused Ub on the N-terminus to bypass the initial priming steps. In every instance, the addition of the $UBE2S^{CTP}$ enhanced the rate of substrate depletion regardless of the initial substrate state (Fig. 2c, Extended Data Fig. 4a).

These results suggest that the $UBE2S^{CTP}$ potentially influences both the APC/C-UBE2C-dependent substrate priming and multiubiquitination. To characterize the first Ub transfer step by APC/C-UBE2C (substrate priming), we blocked multiubiquitination or Ub chain elongation by UBE2C using a single lysine substrate ($cycB^{NTD*}$(1K)) and methylated

ubiquitin (meUb) in a single encounter assay. This experiment allows us to observe the transfer of Ub during a single APC/C^{CDH1}-$cycB^{NTD}$*(1K) binding event. First, APC/C^{CDH1} and $cycB^{NTD}$*(1K) are preincubated in the absence or presence of $UBE2S^{CTP}$. Next, UBE2C~Ub and an excess of unlabeled substrate (600-fold Hsl1) are added simultaneously. Therefore, only $cycB^{NTD}$*(1K) that is pre-bound to APC/C^{CDH1} is modified, and only the initial substrate binding and priming event is observed. Quantification showed that the amount of the monoubiquitinated $cycB^{NTD}$*(1K) formed by APC/C^{CDH1}-UBE2C was indeed at least 3.5-fold higher when the $UBE2S^{CTP}$ was present (Fig. 2d, Extended Data Fig. 4b). In an orthogonal assay that allowed for multiple APC/C^{CDH1}-$cycB^{NTD}$*(1K) binding events, we also showed that modification with the first Ub was more abundant in APC/C^{CDH1}-UBE2C-dependent reactions complemented with $UBE2S^{CTP}$ (Extended Data Fig. 4c). These results point to an unknown mechanism of APC/C-UBE2C activation enhancement that is $UBE2S^{CTP}$-dependent.

UBE2S is a regulator of mitosis. During mitosis, the APC/C is phosphorylated to utilize a different coactivator, CDC20. We examined the effect of the $UBE2S^{CTP}$ on ubiquitination reactions using either a phospho-mimic version of APC/C (APC/C-pE), which can function with CDC20 or CDH1, or a non-phosphorylatable version of the APC/C (APC/C-pA), which can only function with CDH1[40]. The $UBE2S^{CTP}$ enhanced substrate polyubiquitination by every APC/C version tested with both coactivators. (Fig. 2e–f, Extended Data Fig. 4d–e). Therefore, the $UBE2S^{CTP}$ effect is not dependent on a specific state of the APC/C, suggesting that the $UBE2S^{CTP}$ influences polyubiquitination and substrate priming by directly affecting APC/C activation or UBE2C activity.

$UBE2S^{CTP}$ stimulation of APC/C is coactivator independent and harnesses the APC2–APC11 catalytic core for the recruitment and activation of UBE2C~Ub.

Since the enhancement of substrate modification by the $UBE2S^{CTP}$ was observed across multiple substrate, coactivator, and APC/C combinations we can assume that $UBE2S^{CTP}$ either 1) behaves in a manner similar to a canonical coactivator by stimulating APC/C activity or 2) directly stimulates UBE2C~Ub. APC/C coactivators are recruited to the APC/C through an Isoleucine-Arginine (IR) tail at their C-terminus that binds to APC3 and a C-box motif at their N-terminus that binds to APC8[24]. To understand if the $UBE2S^{CTP}$ influences the conformation of the APC2–APC11 catalytic core or if it binds directly to UBE2C, we devised a set of assays to monitor APC/C activation that bypass the need for a coactivator to recruit substrate.

First, to circumvent coactivator-mediated substrate recruitment, we genetically fused the cyclin-B^{NTD} (residues 1-95) to the substrate co-receptor subunit, APC10 (Fig. 3a). Ubiquitination reactions were performed with an APC/C variant that lacks APC10 ($APC^{\Delta APC10}$) and without a coactivator[41]. Ubiquitination of the $CycB^{NTD}$-APC10 fusion was monitored using separate antibodies against APC10 and Ub (Fig. 3b). Reactions which contain $UBE2S^{CTP}$ show a ~3-fold increase in $CycB^{NTD}$-APC10 ubiquitination compared to reactions that lack the $UBE2S^{CTP}$ (Fig. 3c). We hypothesize that the $UBE2S^{CTP}$ triggers ubiquitination in a coactivator-independent manner suggesting a new mechanism of APC/C activation that differs from existing paradigms.

To directly compare coactivator-mediated activation relative to UBE2S^{CTP}-mediated activation, we used an assay that monitors the intrinsic ability of the APC/C^{CDH1} to position and catalyze the discharge of Ub from UBE2C~Ub. Briefly, the catalytic Cys of UBE2C is substituted for Ser to form an oxyester-bonded UBE2C~Ub. Previously, we showed that the hydrolysis of the UBE2C~Ub linkage requires CDH1 to activate the APC/C and the APC2^{WHB} and APC11^{RING} domains to clasp UBE2C~Ub[25]. Similarly, we added wild-type APC/C or an APC/C variant lacking the APC2^{WHB} and APC11^{RING} (APC/C$^{\Delta R\Delta W}$) to the UBE2C~Ub oxyester and followed UBE2C~Ub hydrolysis over time. Remarkably, the APC/C was able to hydrolyze UBE2C~Ub upon the addition of the UBE2S^{CTP} in the absence of CDH1 in a manner still dependent on the APC2^{WHB} and APC11^{RING}. Therefore, the UBE2S^{CTP} facilitates the recruitment of UBE2C~Ub to the APC/C rather than acting on UBE2C directly (Fig. 3d, Extended Data Fig. 5a). Taken together, the APC/C activation mechanism by the UBE2S^{CTP} is coactivator-independent but APC/C-dependent.

To observe the influence of UBE2S-dependent activation of APC/C in cells, we examined the effect of siRNA-mediated knockdown of UBE2S and CDC20 on the mitotic transition (Fig. 3e, Extended Data Fig. 5b–c). By using HeLa cells that stably express H2B-GFP, we identified mitotic cells and measured the mitotic duration using time-lapse microscopy. Unperturbed HeLa cells require a median time of 26 minutes to complete mitosis, measured from the time of nuclear envelope breakdown to anaphase onset. The individual depletion of either UBE2S or CDC20 increased the mitotic duration to 36 minutes and 48 minutes, respectively. Co-depletion of UBE2S and CDC20 caused a significant mitotic delay, with cells requiring a median time of 75 minutes to complete mitosis. U2OS cells that stably express H2B-mCherry showed a similar trend (Extended Data Fig. 5c).

Furthermore, we used a HeLa cell extract system that allows for the measurement of substrate degradation as a readout for APC/C-UBE2C activity. In a UBE2S-depleted cell extract, the substrate degradation rate for Securin and Cyclin B was reduced (Fig. 3f). Addition of a catalytically inactive UBE2S^{C95K} increased the degradation rate of Securin (Fig. 3g, Extended Data Fig. 5d), closely resembling our biochemical data. This suggests that multiple pathways induce the conformational changes for UBE2C~Ub recruitment to the APC/C for substrate polyubiquitination.

The UBE2S^{CTP} rescues an APC/C variant defective in coactivator-dependent activation

Based on our results, UBE2S^{CTP} activation occurs directly on the APC/C**.** One possible explanation for this result is that UBE2S^{CTP}-dependent activation mimics coactivator-induced activation where a conformational change in the catalytic core allows for UBE2C recruitment. Previous studies revealed that the N-terminal WD40 domain of APC1 is necessary for this coactivator-dependent conformational change[26]. These studies show that deletion of the WD40 domain (APC/C$^{\Delta APC1\text{-}WD40}$) locks the APC2–APC11 catalytic core in a “downward” conformation similar to the apo state rendering the UBE2C-binding site inaccessible in the presence of coactivator (Fig. 4a). For UBE2S-mediated ubiquitination, the APC1^{WD40} domain was shown to be dispensable. We confirmed these findings and showed that the addition of the APC1^{WD40} domain *in trans* restores APC/C$^{\Delta APC1\text{-}WD40}$ activation and UBE2C-dependent activity (Extended Data Fig. 6a). Therefore, APC/

$C^{\Delta APC1\text{-}WD40}$ activation for UBE2C-dependent ubiquitination can serve as a readout to distinguish between the active and inactive states of APC/C.

To compare the activity of wild-type APC/C to APC/$C^{\Delta APC1\text{-}WD40}$ in the presence of either UBE2C, UBE2S, or both E2s, we performed ubiquitination assays using an array of substrates (Fig. 4b–e, Extended Data Fig. 6b–d). For both E2s, addition of $UBE2S^{CTP}$ increased substrate turnover and enriched for low molecular weight products (Fig. 4b, Extended Data Fig. 6b, compare lanes 3 and 4). This suggests that the $UBE2S^{CTP}$ rescues UBE2C-dependent Ub ligation but competes with UBE2S to block UBE2S-dependent chain elongation (Fig. 4c, Extended Data Fig. 6c, compare lanes 3 and 4). Strikingly, when UBE2C alone is present, the addition of $UBE2S^{CTP}$ radically increases UBE2C-dependent ubiquitination (Fig. 4d–e, Extended Data Fig. 6d, compare lanes 3 and 4). These effects are conserved amongst several substrates and ablated when the last four residues of $UBE2S^{CTP}$ are changed to alanine ($UBE2S^{CTP-4A}$) (Fig. 4d–e, Extended Data Fig. 6b–d).

To determine the full extent of $UBE2S^{CTP}$ -mediated activation of substrate ubiquitination, we measured the kinetic parameters of ubiquitination by APC/$C^{\Delta APC1\text{-}WD40}$ relative to wild-type APC/C in the presence or absence of the $UBE2S^{CTP}$. UBE2C was titrated into ubiquitination reactions containing Ub-$CycB^{NTD}$*. Product formation (i.e. ubiquitinated forms of Ub-$CycB^{NTD}$*) was quantified and normalized relative to wild-type APC/C^{CDH1} reactions. APC/$C^{\Delta APC1\text{-}WD40}$ activity was reduced by ~70% in its apparent maximum velocity (V_{max}^{app}) compared to wild-type APC/C. When $UBE2S^{CTP}$ was added, the defective V_{max}^{app} was completely restored back to wild-type levels (Fig. 4f, Extended Data Fig. 6e).

A possible explanation for the increase in Ub-$CycB^{NTD}$* ubiquitination by APC/$C^{\Delta APC1\text{-}WD40}$ in the presence of $UBE2S^{CTP}$ is that $UBE2S^{CTP}$ binding alters rather than simply facilitates UBE2C binding to APC/C for Ub transfer to substrates. To survey the chain types formed by both WT APC/C and the APC/$C^{\Delta APC1\text{-}WD40}$ supplemented with the $UBE2C^{CTP}$, we used label-free mass spectrometry of side-by-side polyubiquitination reactions using CDH1 and Securin. After isolation of the Ub_n~Securin product, subsequent proteolysis, and semi-quantitative mass spectrometry analysis of the resultant peptides, we found that the lysines targeted for Ub ligation are similar in all conditions and that K11-, K48-, and K63-linked ubiquitin chains were formed (Extended Data Fig. 6f). Reactions containing APC/$C^{\Delta APC1\text{-}WD40}$ showed decreased levels of total ubiquitination but returned to near wild-type levels with the addition of $UBE2S^{CTP}$ (Fig. 4g).

To dissect the $UBE2S^{CTP}$-mediated activation of APC/$C^{\Delta APC1WD40}$, we used the hydrolysis of oxyester-linked UBE2C~Ub to monitor APC/C activation. CDH1 was insufficient for facilitating the hydrolysis of UBE2C~Ub by APC/$C^{\Delta APC1\text{-}WD40}$ because of its inability to mobilize the APC2–APC11 catalytic core (Fig. 4h, Extended Data Fig. 6g). In contrast, $UBE2S^{CTP}$ alone was sufficient to activate APC/$C^{\Delta APC1\text{-}WD40}$ and induce the hydrolysis of Ub from UBE2C (Fig. 4h). This indicates that the $UBE2S^{CTP}$-dependent conformational change of the APC/C catalytic core occurs through a WD40-independent mechanism that is truly distinct from coactivator-mediated stimulation.

The UBE2S CTP binding to the APC2–APC4 groove activates the APC/C to function with UBE2C

Several APC/C subunits bind peptide motifs. Cryo-EM structures of APC/C bound to UBE2S or EMI1 demonstrate that they are both recruited to a groove composed of APC2 and APC4[24,27,37,38]. UBE2S^{CTP} or related CTPs (EMI1^{CTP} or EMI2^{CTP}) have been shown to be responsible for binding to coactivators and other APC/C subunits[33,35,42]. The N-terminus of the coactivators, where the C box is located, binds to APC8 when activating the APC/C (Fig. 5a)[19,24,43]. Therefore, we sought to understand if UBE2S^{CTP} induces activation of the APC/C by binding to the C-box binding groove on APC8 or the APC2–APC4 groove.

We took multiple approaches to pinpoint the binding surface for UBE2S^{CTP} responsible for APC/C activation. First, we estimated the binding affinity of UBE2S^{CTP} to APC/C by monitoring Securin* ubiquitination using APC/C$^{\Delta APC1\text{-}WD40}$-CDH1, UBE2C, and a UBE2S^{CTP} titration. Modified substrate served as a readout for APC/C activation. We determined the concentration required for half-maximal activation to be 0.87 μM (Fig. 5b, Extended Data Fig. 7a). This value corresponds well with the binding affinity (K_D) of 1.1 μM measured by fluorescent polarization using a fluorescein-labeled UBE2S^{CTP} and the APC/C Platform (composed of APC1, APC2, APC4, APC5, APC11) (Fig. 5c). These results suggest the UBE2S^{CTP} binds to the APC/C Platform.

To differentiate between the activation mechanisms of UBE2S^{CTP} and CDH1, we used APC/C variants with substitutions that block peptide binding to APC8 or the APC2–APC4 groove based on previous studies[24,27]. First, we looked at whether UBE2S^{CTP} can activate APC/C variants harboring mutations on APC8. In the presence of UBE2S^{CTP}, APC/C variants with mutations that result in defective coactivator binding, APC8 N339A:E374R (APC/C^{CBM1}) and APC8 N339A:E410R (APC/C^{CBM2}), showed similar levels of UBE2C~Ub hydrolysis compared to WT APC/C (Fig. 5d, lanes 6-11). Additionally, UBE2S^{CTP} increases substrate ubiquitination by APC/C$^{APC8\text{-}N339A}$-UBE2C (Fig. 5e, Extended Data Fig. 7b, compare lanes 4-5), suggesting that the UBE2S^{CTP}-dependent activation is independent of the APC8 C-box binding groove.

APC4 (APC/C$^{APC4\text{-}D33K}$) blocks UBE2S-dependent chain elongation by preventing UBE2S recruitment to the APC/C[27]. We found that APC/C containing APC4-D33K disrupted UBE2S^{CTP}-dependent UBE2C~Ub hydrolysis (Fig. 5d, lanes 4-5). To further confirm this interaction, we examined the combined effects of the APC1-WD40 deletion and APC4-D33K mutation (APC/C$^{\Delta APC1\text{-}WD40,APC4\text{-}D33K}$) on APC/C activation by UBE2S^{CTP} (Extended Data Fig. 7c–d). Unlike APC/C$^{\Delta APC1\text{-}WD40}$, APC/C$^{\Delta APC1\text{-}WD40,APC4\text{-}D33K}$ is not activated by UBE2S^{CTP} (Fig. 5f). Altogether, UBE2S^{CTP} binding is specific to the APC2-APC4 groove, increasing the rate of UBE2C-dependent ubiquitination.

DISCUSSION

APC/C-mediated Substrate Priming is Enhanced by the Elongating E2 UBE2S

The APC/C is under dynamic yet precise conformational control. Cryo-EM structures have unveiled an array of APC/C conformations in complex with various coactivators, inhibitors, substrates or E2s. These have revealed an ensemble of catalytic states of the APC/C,

reflecting its re-organization throughout the cell cycle. Given the critical role of APC/C and other E3s in numerous biological processes, there remains significant interest in understanding the regulation of transitions between conformational states and how these states drive the formation of diverse ubiquitin chain topologies (reviewed in [4,9,11,13,14]).

APC/C adopts specialized architectures for the direct ligation of Ub to substrate using UBE2C, and for K11-linked ubiquitin chain elongation using UBE2S[24,25,27,35,37]. Formation of multiple, poly- and/or branched ubiquitin chains requires the APC/C to interconvert between diverse architectures. Current models show the APC2-APC11 subunits in different positions depending on whether UBE2C or UBE2S is actively used, preventing use of the other[27]. This reveals a critical shortcoming in our current understanding of the APC/C: how are these architectures coordinated to enable substrate polyubiquitination if both E2s cannot actively transfer Ub at the same time? We address this question through a refined set of enzymatic assays that distinguish between binding and activation events. Remarkably, this analysis reveals that UBE2S, which elongates Ub chains on previously primed substrates, enhances the ability of APC/C to stimulate UBE2C~Ub, the priming E2. This type of reciprocal relationship between the two E2s implies a positive feedback mechanism that ensures efficient substrate ubiquitination by the APC/C (Fig. 6).

In the Apo state, the APC/C is inactive, with the catalytic core (APC2-APC11) positioned down and away from the substrate and unable to bind UBE2C~Ub. Upon activation, triggered by coactivator and substrate binding, the catalytic core moves up and towards the substrate. This exposes the UBE2C binding and activation sites ($APC2^{WHB}$ and $APC11^{RING}$)[19,24,25]. The long-range conformational changes in APC2–APC11 are mediated by $APC1^{WD40}$ and are critical for UBE2C function[42]. We suggest that $UBE2S^{CTP}$ binds directly to the ‘bottom’ of APC2 in the APC2–APC4 groove. This results in increased UBE2C activity (substrate priming and multiubiquitination) in a manner that is functionally similar to what is achieved by coactivators. However, the peptide binding event is mechanistically distinct from coactivator binding: $UBE2S^{CTP}$-dependent activation bypasses the need for the $APC1^{WD40}$ domain. We therefore propose a new model for APC/C activation where UBE2S stabilizes the active conformation of the APC/C by binding to the APC2-APC4 groove, thereby promoting polyubiquitination efficiency.

APC/C uses Multiple Positive Feedback Mechanisms to Increase Substrate Polyubiquitination

UBE2S can only act on substrates previously modified by UBE2C with single Ub or short chains[28–33]. By stimulating APC/C-UBE2C activity, UBE2S accelerates the formation of its own substrate. Previously, CDC20 was shown to assist in the recruitment of UBE2S to the APC/C[44]. This suggests that the close relationship between the coactivator and UBE2S facilitates substrate priming by UBE2C. A second mechanism, PAA, involves substrate-linked Ub binding directly to the APC/C to enhance processive polyubiquitination[27,34]. Together, these mechanisms work in sync to increase substrate polyubiquitination while allowing for the APC/C to flexibly adopt distinct ubiquitination architectures.

It is interesting to speculate that these mechanisms are critical during the rapid transitions in the cell cycle where APC/C-dependent substrate polyubiquitination may need a boost. For

example, the Mitotic Checkpoint Complex (MCC) restrains APC/C activity in mitosis until the spindle checkpoint is satisfied[17]. Yet the UBE2S^{CTP}-binding groove is still accessible and UBE2S can bind to APC/C-MCC. This potentially keeps the APC/C poised to swiftly transition the cell out of mitosis upon checkpoint silencing[45,46]. In support of this prediction, the depletion of UBE2S prolonged mitosis in HeLa, U2OS and RPE cells[31,35]. The UBE2S^{CTP}-binding groove therefore serves as another regulatory aspect of the cell cycle that could be an amenable target for therapeutics[47]. More broadly, understanding the regulatory mechanisms that amplify E3 activity will assist in the investigation of compounds that target protein destruction[48].

Broad Implications for RING E3-E2-E2 Mechanisms

A recurring theme in the regulation of ubiquitin ligases is rearrangement of the active site from an inactive or autoinhibited state to an active state through post-translational modifications or protein-protein interactions to prevent off-target ubiquitination[4]. APC/C is inactive until it binds a coactivator[19,24,25]. In mitosis, phosphorylation of an autoinhibitory loop on APC1 allows CDC20 to bind[40,49,50]. For cullin-RING ligases (CRLs), ligase activity requires the reversible conjugation of the Ub-like protein NEDD8 to the cullin which catapults the RING domain towards the substrate to allow E2~Ub activation and recruitment[51]. Several RBRs have also been shown to be autoinhibited and freed for activity via post-translational modifications and protein binding[4]. For example, the E3 RBR ARIH1 works with Nedd8-conjugated CRLs in a tag team to generate a nonlinear Ub cascade[52,53]. Also, cIAP1(BIRC2), a RING E3 that regulates programmed cell death, relies on the second mitochondrial activator of caspase (SMAC) peptide to induce a conformational rearrangement that stimulates E3 function[54,55]. For the APC/C, E3 activation comes from the UBE2S^{CTP}. As ~40% of E2s have N- or C-terminal extensions and several E3s use multiple E2s, understanding how these E2s ensure precise tuning of the ubiquitination signal and their biological consequences will require a thorough examination of all of the enzymes involved[56].

For several E3s that work with multiple E2s, a hand-off or sequential transfer mechanism has been proposed. Direct ligation to the substrate, or priming, is carried out by the first E2 while Ub chain elongation occurs using a second E2[7,9,57]. Therefore, it is possible that these chain-elongating E2s feedback into the initial steps. For example, SCFs work with UBE2R1 (CDC34) for Ub chain elongation[8,53]. Like UBE2S, UBE2R1 has a highly charged tail that binds to the cullin surface[58]. Future studies are needed to uncover how the high-affinity, dynamic E2 extension-E3 interactions regulate E3 function, influence the initial activation and priming ubiquitination steps, and alter the ubiquitination signal. Inversely, could the binding of the priming enzymes also activate chain elongation through conformational rearrangement? Evidence of this may already exist from a seminal study of the yeast Ub-fusion degradation (UFD) pathway where the presence of the initiating enzyme (UFD4) was also required for the chain elongation by UFD2[59].

In summary, the traditional view of a ubiquitin cascade involves the linear transfer of Ub from the E1 to the E2 to the E3-substrate, with the E2s viewed as inert Ub carriers activated by or handing off their Ub to the E3. However, the E2 UBE2S continues to demonstrate that

such models can be misleading and are insufficient. UBE2S does not use the RING domain in a traditional sense and it activates the E3 APC/C to accelerate the formation of its own substrate, that is, substrate-linked Ub. This establishes an interdependence between the substrate priming and Ub-chain elongation steps which were previously described as independent and unconnected events. We have shown that the Ub cascade leads to a more complex and intertwined mechanism than anticipated. Further study will provide a thorough understanding of how the myriad of enzymes involved in the Ub cascade are successfully integrated in the regulation of cellular processes.

MATERIAL AND METHODS

Protein purification

Wild-type and mutant versions of the components necessary for APC/C-dependent ubiquitination and binding assays (Human APC/C, CDH1, CDC20, UBA1, UBE2C, UBE2S, and substrates) were expressed and purified largely as previously described[25,27,37,45,60]. Recombinant APC/C (wild-type and mutants), its Platform (containing subunits APC1, APC2, APC4, APC5, APC11) subcomplex, UBA1, CDH1, and CDC20 were expressed using a baculovirus expression system. All other proteins were expressed in BL21-Codon Plus (DE3)-RIL cells.

APC/C complexes were expressed with a twin-Strep tag at the C-terminus of APC4 and purified by affinity chromatography with Strep-Tactin Sepharose and elution with desthiobiotin, anion exchange and size exclusion chromatography (SEC)[37,60]. Unless otherwise specified, all SEC was performed in a final buffer of 20 mM Hepes pH 8, 200 mM NaCl, and 1 mM DTT.

CDH1 was expressed with an N-terminal 3xMyc-His_6 tag and purified using nickel affinity chromatography[37,40,60]. Following HRV 3C protease treatment, CDH1 was further purified by cation exchange chromatography and SEC 20 mM HEPES pH 7, 300mM $AmSO_4$, and 1mM DTT. CDC20 was purified by anti-Flag-affinity gel and subsequent elution by the addition of FLAG peptide[40,45]. The N-terminal 3xFlag-tag was removed by HRV 3C protease-mediated cleavage and purified by cation exchange chromatography and SEC.

Wild-type UBE2S and mutants (except for the $UBE2S^{CTP}$) were expressed with an N-terminal multipurpose composite tag from a customized pRSF duet vector[37]. This tag consists of an His_6 tag, TEV protease site, FLAG tag, and HRV 3C protease site. Tagged UBE2S and variants were purified by nickel affinity chromatography, followed by HRV 3C protease-mediated cleavage, ion exchange, and SEC.

UBE2C, wild-type and C114S, were purified by nickel affinity chromatography and SEC[25,37]. For substrate-independent assays, the C114S-substituted UBE2C was charged by adding UBA1, Ub, and MgATP. After overnight incubation at 30ºC, the oxyester-linked UBE2C~Ub was purified from the other reaction components by SEC.

The substrates in ubiquitination assays - $CycB^{NTD}$* (residues 1-95), Ub-$CycB^{NTD}$*, Securin*, Ub-Securin* - were expressed as N-terminal GST-TEV and C-terminal Cys-His_6

fusions (* denotes fluorescently labeled)[37,60,61]. The substrates were purified by glutathione-affinity chromatography, treated with TEV protease to cleave off the GST tag, and further purified by nickel-affinity chromatography. Substrates were then labeled with fluorescein-5-maleimide on its single cysteine. The reaction was quenched with DTT, buffer exchanged by Nap5 columns, and further purified by SEC. CyclinA and the $CycB^{NTD}$-1K mutant, a construct that contains residues 1-88 and a single lysine (Lys64) – all other lysine residues were substituted to arginine except for Lys64- were expressed as a N-terminal GST fusion, purified by glutathione-affinity chromatography, treated with TEV and further purified by SEC[27,45]. Both the Cyclin A and $CycB^{NTD}$-1K mutant substrates contain an additional Strep-tag after the TEV cleavage site. Cyclin A and the $CycB^{NTD}$-1K mutant were fluorescein-labeled with sortase. After TEV cleavage, 10 μM of $CycB^{NTD}$-1K and Cyclin A were subjected to 150 nM Sortase and 1 mM LPETGG peptide in 10 mM HEPES pH 8, 50 mM NaCl, and 10 mM $CaCl_2$. After 30 min incubation at room temperature the reactions were quenched with 50 mM EDTA and then purified by Strep-Tactin Sepharose, eluted with desthiobiotin, and further purified by SEC. The $CyclinB^{1-95}$-APC10 fusion was purified by glutathione-affinity chromatography using a N-terminal GST tag. The protein was further purified by cation-exchange chromatography and SEC.

E1 (UBA1) was expressed with an N-terminal GST tag. After purification by glutathione-affinity chromatography, UBA1 was treated with Thrombin protease and 10mM $CaCl_2$. UBA1 then underwent anion exchange chromatography and SEC.

Ub used in substrate ubiquitination assays was purified as previously described[62]. When indicated, Ub was reductively methylated as previously described and purified by SEC[63].

Peptide Synthesis

Ac-KKLAAKKKTDKKRALRRL-NH_2 and Ac-KKLAAKKKTDKKRAAAAA-NH_2 were synthesized using Fmoc chemistry SPPS on PTI Symphony peptide synthesizer. The peptides were synthesized at 25 μmol scale on ChemMatrix Rink amide resin, using 2 × 20 min couplings with 5 eq of amino acids, HATU coupling reagent and 15 equivalents of N-methylmorpholine in DMF. For Fmoc deprotection resin treated twice with 20% piperidine in DMF (3 min and 17 min). N-terminal amino acids were acetylated by 30 min treatment with 10 eq acetic anhydride and N-methylmorpholine in DMF. After synthesis resins were vacuum dried overnight. The peptides were cleaved from the resins by 2h treatment with 2 ml of 2.5% water, 2.5% TIS in TFA, precipitated from cold diethyl ether, separated by centrifugation and washed 3 times with cold ether. The peptides were air dried for a few minutes, dissolved in 50% acetonitrile and lyophilized. Crude peptides were purified by RP HPLC on Waters 1525 pep. HPLC system using SymmetryShield RP-18 column and analyzed by MALDI-TOF MS and analytical HPLC.

Enzyme Assays

Briefly, all ubiquitination assay reactions were prepared by mixing ubiquitination components in assay buffer (20 mM Hepes pH 8, 200 mM NaCl) on ice, warming them up to room temperature and initiating them by the addition of ubiquitin. Next, reactions were quenched with SDS loading buffer at designated time points and separated by SDS-PAGE.

To visualize unmodified substrates and products formed, gels were scanned for fluorescence by using the Amersham Typhoon 5. Substrates and products formed were measured and quantified with ImageQuant software and analyzed with GraphPad Prism. Negative control reactions in enzyme assays consisted of all reaction components involved minus the addition of APC/C.

Ubiquitination assays monitoring the rate of substrate depletion in the presence of UBE2C and a titration of UBE2S (Fig. 1b–c, Extended Data Fig. 2) were performed with 100 nM APC/C, 5 μM UBE2C, 1 μM E1, 250 μM Ub, 6 μM $CycB^{NTD}$*, and 0-10 μM gradient of UBE2S (0, 0.1, 0.5, 1, 5, and 10 μM). Similarly, ubiquitination assays monitoring substrate depletion in the presence of UBE2C and UBE2S variants were performed with 100 nM APC/C, 5 μM UBE2C, 1 μM E1, 250 μM Ub, 6 μM $CycB^{NTD}$*, and 5 μM of UBE2S variants (Figure 2b–c, Extended Data Fig. 3a,d). Bands corresponding to unmodified substrate in these assays were quantitated and normalized to reaction at time zero. Ubiquitination reactions assessing $UBE2S^{CTP}$-dependent activation as an effect amongst various APC/C substrates and APC/C variants were performed as above with the exception that 10 μM $UBE2S^{CTP}$ was used (Figure 2c, Figure 2e–f, Extended Data Fig. 3, Extended Data Fig. 4).

Ubiquitination assays using meUb and fluorescently labeled substrate with a single lysine were performed to assess the role of $UBE2S^{CTP}$ in UBE2C-dependent substrate priming (Figure 2d, Extended Data Fig. 4b). Single encounter experiments (Figure 2d) were used to examine ubiquitination of substrate occurring during a single substrate binding event on APC/C[27]. This was monitored by using a fluorescein-labeled substrate (cycB-NTD*) and excess unlabeled Hsl1, such that APC/C^{CDH1} dissociated from labeled substrate is rapidly sequestered with unlabeled substrate. Briefly, reactions components were prepared in two independent mixes. The first mix, APC-substrate, consisted of APC/C, CDH1, cycB-NTD*(1K), $UBE2S^{CTP}$ or $UBE2S^{CTP-4A}$. This was incubated on ice for 30 min. The second mix, E2-Ub, consisted of E1, E2, MgCl2, ATP, and 600-fold excess of unlabeled Hsl1. Methylated-Ub was added to the second mix 5 min before completion of the 30 min incubation of APC-substrate mixture. Both mixes were allowed to reach room temperature for 5 min. Immediately, both reactions were comixed and quenched at 3 min. Final concentration of all components after initiating reactions were: 100 nM E1, 200 nM APC/C, 0.5 μM CDH1, 80 nM cycB-NTD*(1K), 48 μM Hsl1, 10 μM $UBE2S^{CTP}$ or $UBE2S^{CTP-4A}$, 320 μM meUb. A control reaction identified as ‘no encounter’ was done similarly by swapping the addition of cycB-NTD*(1K) to E2~Ub mix and Hsl1 to APC/C-substrate mix (Extended Data Fig. 4b). Multiple turnover reactions were performed at 100 nM APC/C, 1 μM CDH1, 200 nM UBE2C, 1 μM E1, 125 μM UB, 200 nM cycB-NTD*(1K), and 10 μM $UBE2S^{CTP}$ (Extended Data Fig. 4c). Bands corresponding to primed substrate and unmodified substrate were quantitated. Values were plot as a fraction of primed substrate to unmodified substrate over time.

A dual color assay was used to monitor the role of $UBE2S^{CTP}$ in substrate ubiquitination independently of coactivator (Figure 3b-c)[41]. Briefly, a GST-APC10-CycB-NTD fusion was generated to link residues 1-95 of CyclinB to the C-terminus of GST-fused APC10. This GST-APC10-CycB fusion was added at 1μM to 20 nM APC that lacks the APC10 subunit

along with either reaction buffer or 10 μM UBE2S^{CTP} to a prepared mixture containing 1 μM E1, 5 mM ATP-$MgCl_2$, and 200 nM UBE2C. The mixture was allowed to equilibrate to room temperature and ubiquitin was added at 125 μM to start the reaction. Samples were taken throughout a time course and then analyzed via western blot using either α-Ub (sc-20989, rabbit) or α-APC10 (sc-8017, mouse) antibodies. Secondary antibodies from Invitrogen (goat anti-rabbit 488 35552 and goat anti-mouse 633 A21052) were used to develop protein bands (Figure 3b). Bands were quantified from the α-Ub blot to determine the extent of ubiquitination (Figure 3c).

Qualitative assays probing for the role of UBE2S^{CTP} on APC/C^{CDH1} and UBE2C-dependent activity were performed with 200 nM APC/C or APC/C$^{\Delta APC1WD40}$, 1 μM E1, 1 μM CDH1, 0.2 μM substrate, 0.2 μM UBE2C, 10 μM UBE2S^{CTP}, and 125 μM Ub. Substrates consisted of CycB^{NTD}*, Ub-CycB^{NTD}*, Securin*, Ub-Securin* and *CycA. Reactions were quenched at 10 min (Figure 4b–e, Extended Data Fig. 6b–d).

Experiments measuring the extent of APC/C$^{\Delta APC1\text{-}WD40}$ activation in the presence of UBE2S^{CTP} were carried out using 20 nM APC/C, with 1 μM E1, 1 μM CDH1, 0.2 μM substrate, 10 μM UBE2S^{CTP}, 125 μM Ub, and a range of 0.05 to 5 μM UBE2C (Figure 4f, Extended Data Fig. 6e). Reaction kinetics were plotted and fit using Michaelis-Menton Kinetics and GraphPad Prism.

Reactions that were analyzed by mass spectrometry analysis were performed at 100 nM APC/C WT or APC/C$^{APC1\Delta WD40}$, 1 μM UBE2C, 1 μM E1, 5 μM His_6-tagged Securin*, 150 μM Ub, and 50 μM UBE2S^{CTP} (Figure 4g). These reactions were quenched at indicated time points with a final concentration of 4M Urea. Unmodified and modified His_6-tagged Securin was isolated by a nickel pulldown and eluted with PBS containing 250 mM imidazole.

Assay to measure the activation kinetics of UBE2S^{CTP} with APC/C, substrate ubiquitination reactions were performed with APC/C$^{\Delta APC1\text{-}WD40}$ at 20 nM with 1 μM E1, 1 μM CDH1, 0.2 μM Securin*, 0.2 μM UBE2C, and 0.3 nM to 10 μM UBE2S^{CTP} (Figure 5b, Extended Data Fig. 7a).

To assess the effect of APC8 mutations, known to block CDH1 binding, on UBE2S^{CTP}-dependent activation of APC/C-UBE2C, ubiquitination reactions were performed with 20 nM APC/C or APC$^{APC8\text{-}N339A}$, 0.5 μM E1, 1 μM CDH1, 0.2 μM Ub-CycB^{NTD}*, 0.2 μM UBE2C, 10 μM UBE2S^{CTP}, and 125 μM Ub (Figure 5e, Extended Data Fig. 7b). To assess the effect of APC4-D33K mutation in the rescue of APC/C$^{\Delta APC1\text{-}WD40}$, ubiquitination assays were performed with 1 μM E1, 0.2 μM UBE2C, 0.4 μM Securin* or CycB^{NTD}*, 1 μM CDH1, 100 nM APC/Cs, 10 μM UBE2S^{CTP} or indicated concentrations of UBE2S, and 125 μM Ub (Figure 5f, Extended Data Fig. 7c).

Fluorescence polarization assay

To measure the binding affinity of UBE2S^{CTP} to APC/C Platform, 125 nM fluorescein-labeled UBE2S^{CTP} (*UBE2S^{CTP}) was mixed with a titration of APC/C Platform ranging from 0 to 10 μM (Figure 5c). At 5 min of incubation, fluorescence polarization was

measured using a fluorescence polarimeter with a 505-nm filter in place. Values were fitted in GraphPad Prism.

Substrate independent assay for APC/C activation of UBE2C, monitoring hydrolysis of oxyester-linked analog of UBE2C~Ub

To study the role of UBE2S^{CTP} in its ability to induce an activating conformation of the APC/C, we monitor the ability of APC/C to hydrolyze Ub from UBE2C~Ub in discharge assays (Figure 3d, Extended Data Fig. 5a, Figure 4h, Extended Data Fig. 6g, Figure 5d). Briefly, Ub oxyester-linked UBE2C(C114S) was mixed with either APC/C WT or APC/C variants in the presence or absence of CDH1, and in the presence or absence of UBE2S^{CTP}. Reactions were carried out at 30°C. Reaction mixtures consisted of 1 μM APC/C, 5 μM UBE2C~UB and 1 μM CDH1 or 10 μM UBE2S^{CTP}. After quenching, reactions were separated by SDS-PAGE and products were visualized by Sypro or Coomassie staining. Percent of remaining E2~Ub was calculated, graphed and analyzed with GraphPad Prism. For statistical analysis one-way ANOVA test was applied (DF: 5, F: 108.9, $p<0.0001$) followed by Tukey's multiple comparison test.

Live cell imaging

To study the influence of UBE2S in APC/C-UBE2C activation in cells we monitored cell mitosis transition in HeLa cells stably expressing histone H2B-GFP (a gift from Edward Salmon) and U2OS cells expressing H2B-mCherry and PCNA-mTurquoise2 (PCNA not imaged) (Figure 3e, Extended Data Fig. 5b–c). All cells were negative for mycoplasma and were authenticated. Cells were grown in DMEM (Sigma-Aldrich), supplemented with 10% fetal bovine serum (FBS) (Sigma) and penicillin/streptomycin 1× (Gibco) at 37°C with 5% CO_2. Cells were seeded at 40-30k per well in 12 well glass bottom culture dishes (#1.5, Cellvis). Twenty-four hours prior to microscopy experiments cells were transfected with siRNA by using RNAiMAX Transfection reagent (Life Technologies) according to manufacturer protocol: 0.5nM anti-Cdc20 (Thermofisher D-003225-10, D-003225-12, D-003225-13, and D-003225-27), 9.5nM anti-Ube2s (3'UTR Dharmacon; ORF Qiagen) and anti-Luciferase (Life Technologies). Before the experiment the growing media was replaced with imaging media, FluoroBrite DMEM (Gibco), supplemented with 10% FBS, 4mM L glutamine (Corning), and penicillin/streptomycin. Live cells were observed for 24 h (24-48 h post transfection).

Fluorescence widefield imaging was performed using a Nikon Ti Eclipse inverted microscope with a Plan-Apochromat dry objective lens 20× (NA 0.75) and fluorescence filters (Chroma) - GFP - 470/40 nm; 495 nm; 525/50 nm and mCherry - 545/25nm; 565 nm; 605/70 nm. Images were captured using Andor Zyla 4.2 sCMOS detector (12 bit) and NIS-Elements AR software. Image and data analysis were performed with Python 3.7.1, Numpy, Pandas, Scipy libraries and GraphPad Prism v8. Analyzed data come from three (HeLa) or two (U2OS) independent sets of transfections. Mitotic cells were identified and the time from metaphase to anaphase transition was defined manually. For statistical analysis a non-parametric ANOVA test was applied (Kruskal-Wallis Test) followed by Dunn's multiple comparison test.

APC/C-substrate degradation assay in G1 HeLaS3 extracts.

Confluent HeLaS3 were seeded in 15 cm plates at 3 million cells per plate. Next morning, cells were transfected with 20 nM of two different UBE2S siRNAs using Lipofectamine RNAiMAX reagent (Life Technologies) following the manufacturer's instructions[33]. After 8 h, 2 mM thymidine was added to the medium for 24 h, after which cells were washed with warm PBS once, twice with DMEM and released for 4 h before being treated with 100 ng/ml of nocodazole in DMEM for 11 h. In order to obtain a G1 population, cells were washed as described previously and released for 2 h before harvest. Extract preparation was performed essentially as described[64,65]. The resulting G1 extracts were supplemented with energy mix, ubiquitin, and the indicated amounts of recombinant UBE2S. Reactions were incubated at 30°C, stopped with sample buffer, boiled and analyzed by SDS-PAGE and western blot.

Proteomics – Label-free analysis of his_6-tagged-Securin affinity-purification

For mass spectrometry (Figure 4g), samples were subjected to reduction (5 mM tris (2-carboxyethyl)phosphine (TCEP) for 10 min at room temperature) and alkylation (25 mM chloroacetamide for 20 min at room temperature) followed by single-pot solid-phase-enhanced sample preparation (SP3) protein clean-up[66]. Samples were briefly dried and resuspended in 30 µl digestion buffer (100 mM triethyl ammonium bicarbonate pH 8.5, 0.1% RapiGest) and digested for 2 h at 37°C with Lys-C (0.25 µg) and then a further 6-8 h with trypsin (0.5 µg) at 37°C. The sample were acidified with equal volume of 1% formic acid (FA) to a pH ~ 2, incubated for 15 min, vacuum centrifuged to near dryness and subjected to C18 StageTip desalting.

Label-free analysis was performed in triplicate and analyzed sequentially by LC/MS^2 on a Q Exactive mass spectrometer (Thermo Fisher Scientific) coupled with a Famos Autosampler (LC Packings) and an Accela600 LC pump (Thermo Fisher Scientific). Peptides were separated on a 100-µm i.d. microcapillary column packed with ~0.5 cm of Magic C4 resin (5 µm, 100 Å; Michrom Bioresources) followed by ~20 cm of Accucore C18 resin (2.6 µm, 150 Å; Thermo Fisher Scientific). Peptides were separated using a 75-min gradient of 5-28% acetonitrile in 0.125% FA with a flow rate of ~150 $nL.min^{-1}$.

The scan sequence began with an MS^1 spectrum (Orbitrap analysis; resolution 70,000 at 400 Th; mass range 350−1400 m/z; automatic gain control (AGC) target 3×10^6; maximum injection time 240 ms). Precursors for MS2 analysis were selected using a Top10 method. MS^2 analysis consisted of Higher-energy C-trap dissociation (AGC 1.0×10^5; isolation window 1.2 Th; normalized collision energy (NCE) 27; maximum injection time 118 ms). Precursors with charge state unassigned or different than 2, 3, 4 or 5 were excluded, peptide match option was set to preferred, isotopes were excluded, and previously interrogated precursors were excluded using a dynamic window (set to automatic), minimum AGC target 2×10^3.

Mass spectra were processed using Protein Discoverer version 2.2 (Thermo Fisher Scientific) using the Minora algorithm (set to default parameters). The identification of proteins was performed using the SEQUEST-HT engine against the UniProt Human

Reference Proteome (2017), supplemented with the recombinant Securin sequence and in-house curated sequences of common contaminant proteins. The following parameters were used: a tolerance level of 20 ppm for MS^1 and 0.03 Da for MS^2 and false discovery rate of the Percolator decoy database search was set to 1%. Trypsin was used as the digestion enzyme, three missed cleavages were allowed, and the minimal peptide length was set to 6 amino acids. The carbamidomethylation (+57.021 Da) of cysteine was set as a fixed modification, and the oxidation (+15.995 Da) of methionine, GlyGLy (+114.043 Da) modification of Lysine were allowed as a variable modification as well as protein N-terminus Acetylation (+42.011 Da). Scoring and localization of GlyGly site was done using the ptmRS node (default settings). Protein and peptide were quantified based on the precursor abundance area and only peptides quantified in all three replicates were considered for further analysis. Protein or peptide quantification values were exported for further analysis in Microsoft Excel and GraphPad Prism (v8).

Extended Data

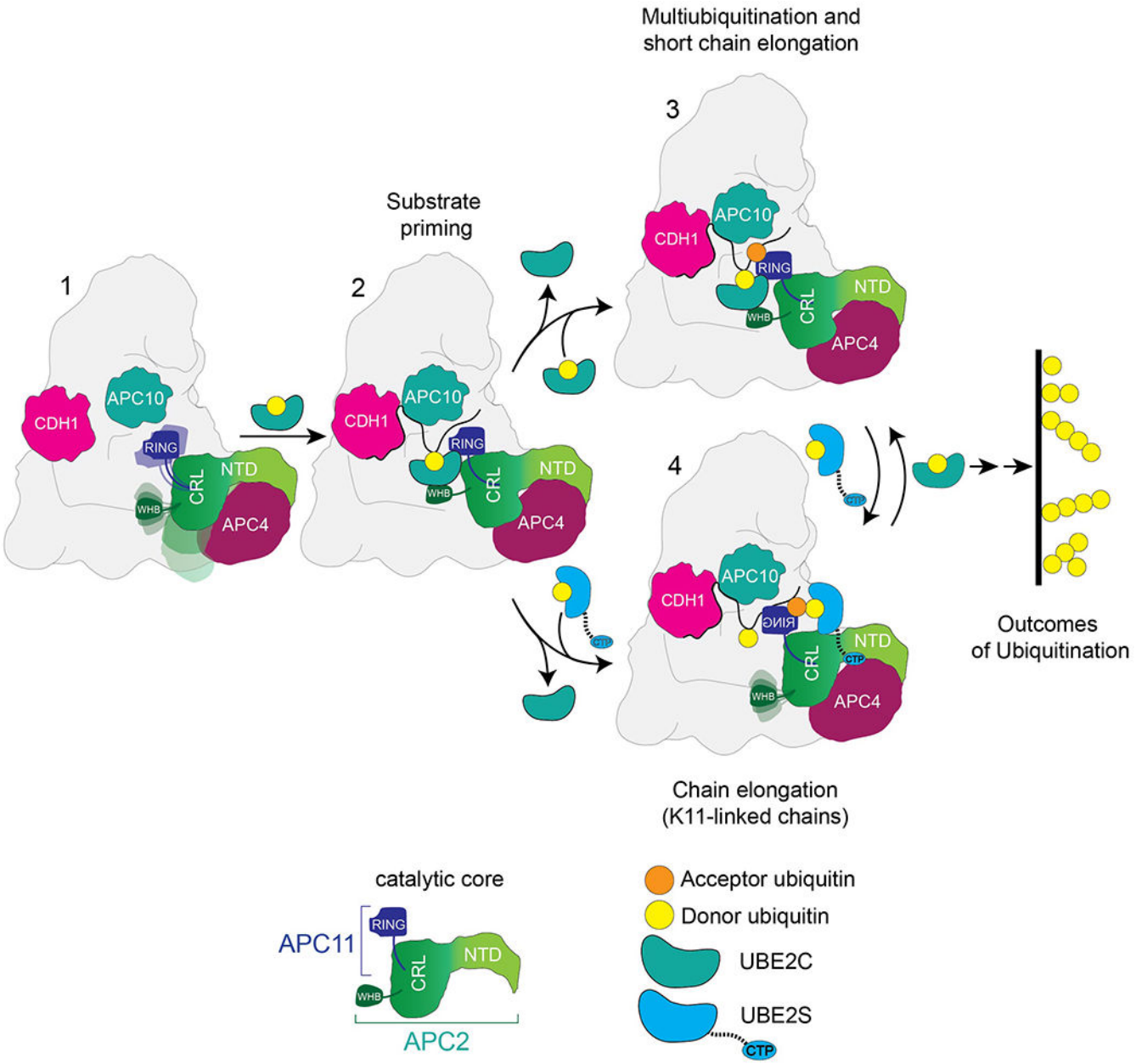

Extended Data Fig. 1. Current model of structural architectures of APC/C^{CDH1}–UBE2C and APC/C^{CDH1}–UBE2S.

Schematic depicting the interplay of substrate ubiquitination mechanisms, including substrate priming, multiubiquitination, and Ub chain elongation, by APC/C^{CDH1}, UBE2C, and UBE2S. Upon APC/C activation by CDH1 binding, catalytic core APC2^{WHB}–APC11^{RING} is mobile and exposed for UBE2C recruitment (1). APC/C^{CDH1}–UBE2C structural architecture for substrate priming and multiubiquitination (2 and 3). APC/C^{CDH1}–UBE2S structural architecture where APC11^{RING} is repurposed and binds acceptor ubiquitin for K11-linked Ub chain elongation (4).

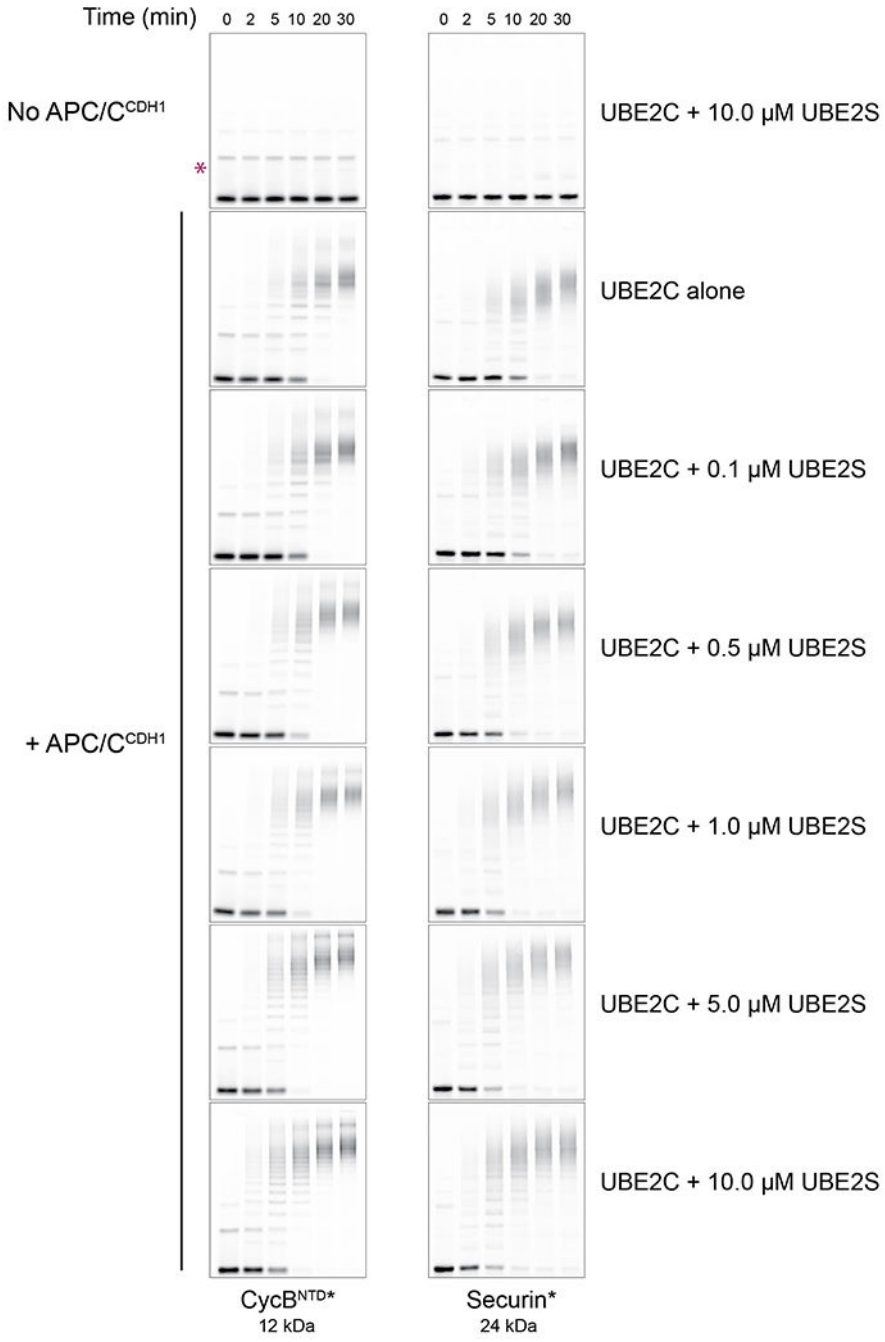

Extended Data Fig. 2. Substrate polyubiquitination assays by APC/C^{CDH1}, UBE2C, and UBE2S.
UBE2S extends Ub chains on substrates, CycB^{NTD}* and Securin*, and increases the rate of substrate modification in a dose-dependent manner. Fluorescence scan of full SDS-PAGE gels used in (**1b**). * Represents contaminant present in substrate stock. Uncropped images are available as source data.

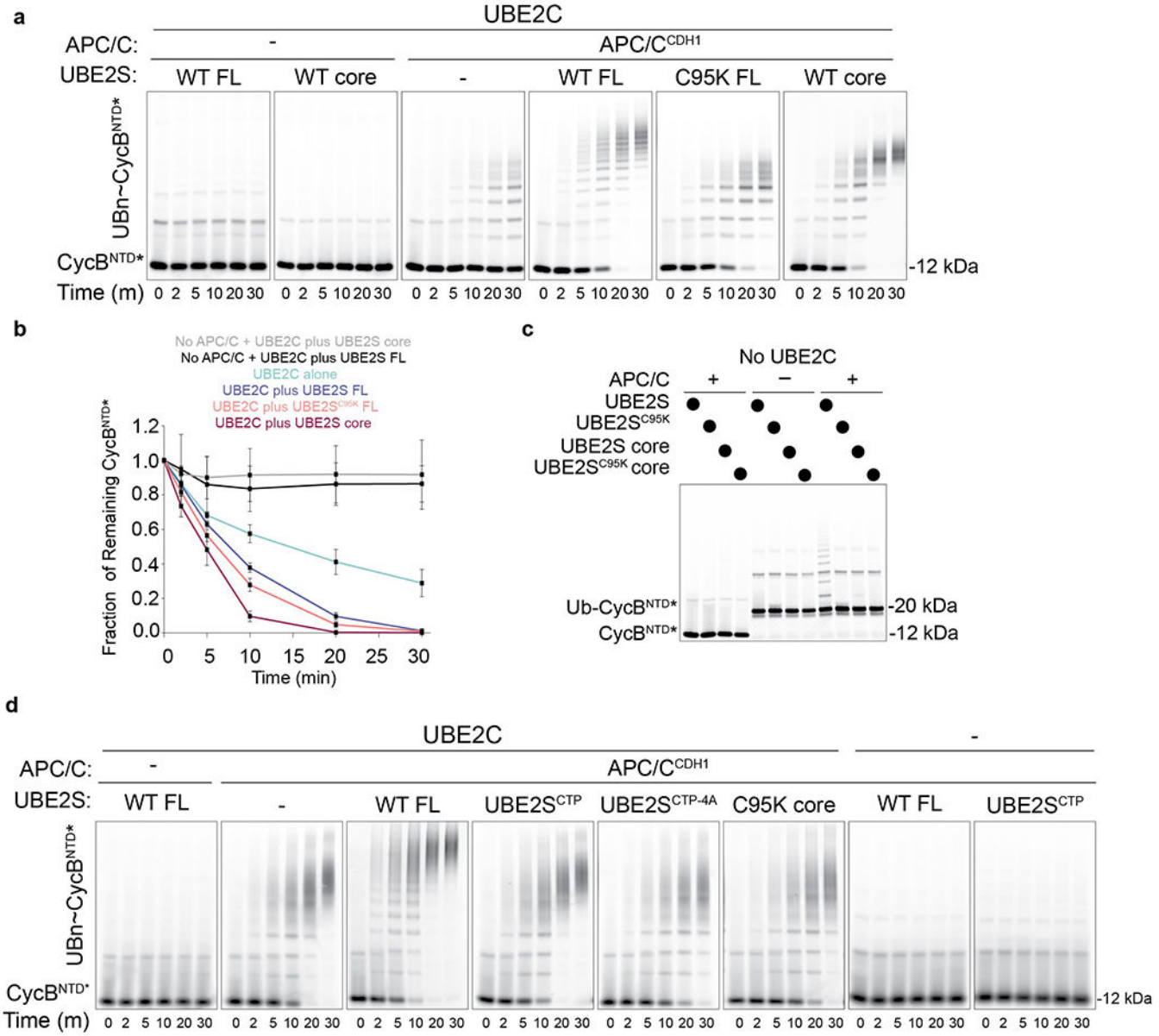

Extended Data Fig. 3. UBE2S^{CTP} increases substrate modification by APC/C^{CDH1}–UBE2C.

a, Catalytically inactive UBE2S^{C95K} enhances rapid turnover of CycB^{NTD*} by the APC/C^{CDH1} and UBE2C. [b], Quantification depicts relative fraction of remaining unmodified CycB^{NTD*} shown in **Extended Data Figure Fig. 3a**. Average of n=3 independent experiments ± s.e.m. **c**, UBE2S UBC domain (UBE2S core) is defective for Ub chain elongation in an APC/C-dependent manner. **d**, UBE2S^{CTP} enhances the rapid turnover of CycB^{NTD*} by the APC/C^{CDH1} and UBE2C. Fluorescence scan of full SDS-PAGE gels used in (**2b**). Uncropped images for panels (**a,c-d**) and data for the graph in (**b**) are available as source data.

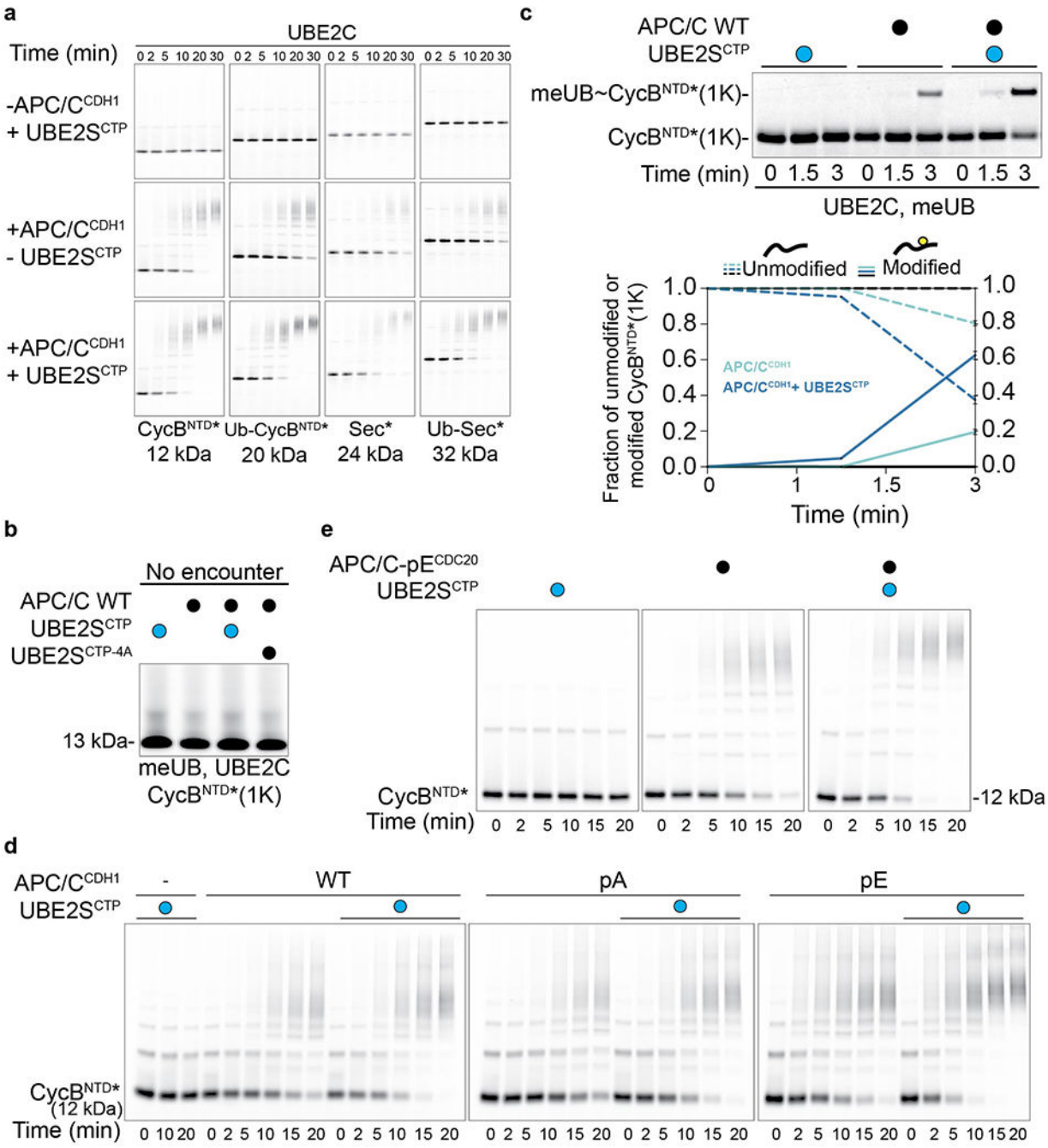

Extended Data Fig. 4. UBE2S^{CTP} accelerates substrate modification in every UBE2C-dependent ubiquitination reaction condition using multiple substrates, APC/C variants, and different coactivators.

a, Fluorescence scan of full SDS-PAGE gels used in (**2c**) showing the effect of the UBE2S^{CTP} on the polyubiquitination of multiple substrates, CycB^{NTD*}, Ub-CycB^{NTD*}, Securin*, Ub-Securin*, by APC/C and UBE2C. **b**, "No encounter" control assay done as in (**2d**) with the exception of swapping fluorescent substrate and cold substrate in the mixtures to prevent a reaction to occur. **c**, Ubiquitination reaction monitoring role of UBE2S^{CTP} on UBE2C-dependent APC/C substrate priming using a single lysine substrate, CycB^{NTD*}(1K),

and methylated Ub (meUb). The unmodified substrate and monoubiquitinated product are followed over time in the absence or presence of UBE2SCTP. Quantitation shows effect of UBE2SCTP on substrate priming by APC/C^{CDH1}-UBE2C, graphs depicts fraction of unmodified substrate and meUb~$CycB^{NTD*}$(1K) over time. Average of n=3 independent experiments ± s.e.m. **d**, UBE2C-dependent substrate turnover is accelerated by UBE2SCTP when non-phosphorylated, APC/C-pA, or phopho-mimetic APC/C, APC/C-pE, is used. Fluorescence scan of full SDS-PAGE gels used in (**2e**). **e**, Substrate turnover by phosphomimetic APC/C, APC/C-pE, and CDC20 is enhanced by the addition of $UBE2S^{CTP}$ in UBE2C-dependent reactions. Fluorescence scan of full SDS-PAGE gels used in (**2f**). Uncropped images for panels (**a-e**) and data for the graph in (**c**) are available as source data.

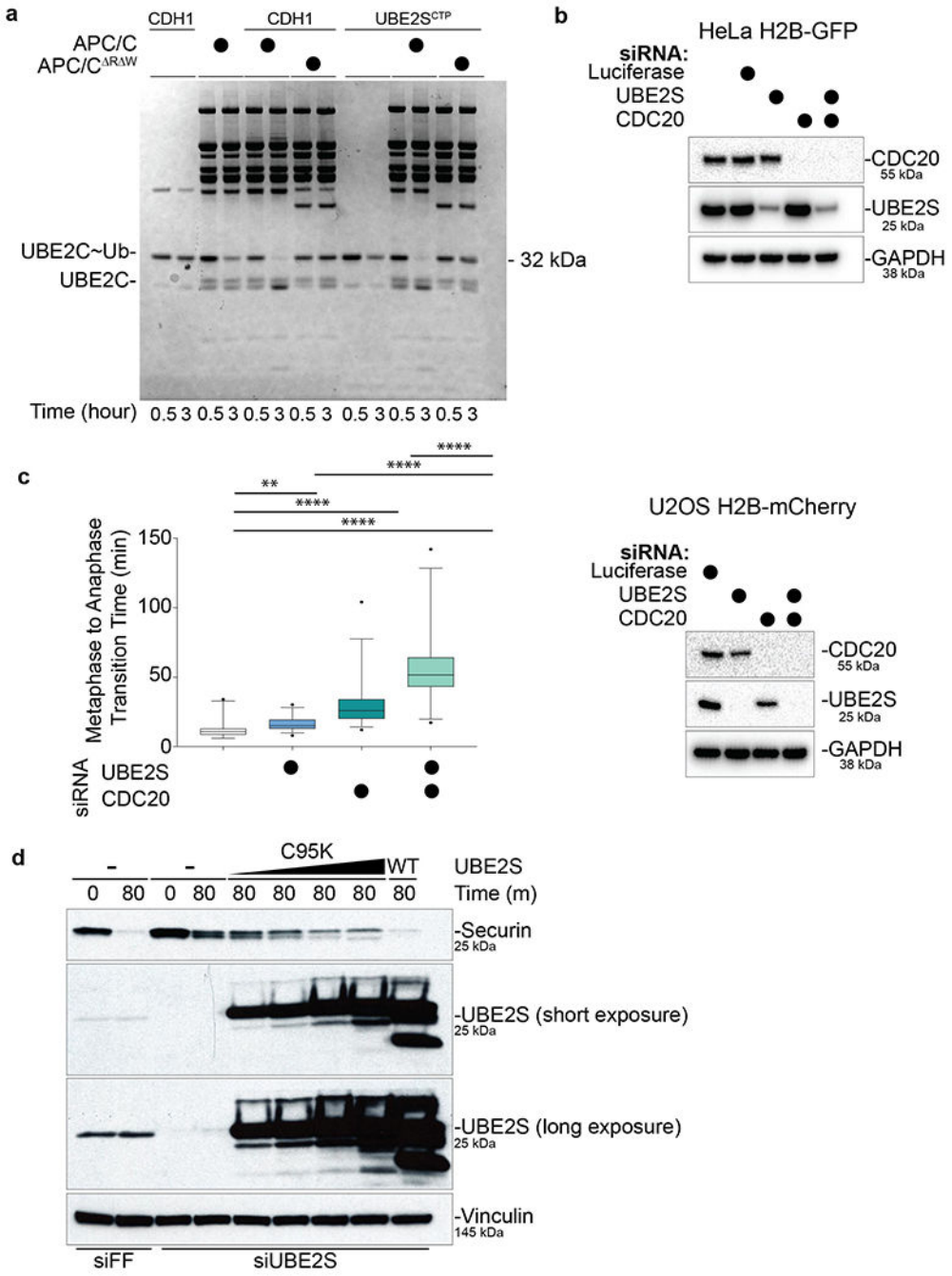

Extended Data Fig. 5. UBE2S^{CTP} stimulates the APC/C to activate UBE2C~Ub hydrolysis.

a, UBE2S^{CTP} promotes a substrate-independent APC/C activation of UBE2C, monitored by the hydrolysis of UBE2S~Ub over time into UBE2C and Ub. Detected using Coomassie-stained gels, full gel from (**3d**). **b**, Western blot of (**3e**) showing successful knockdown of UBE2S and CDC20 in HeLa H2B-GFP. **c**, Time necessary for the metaphase to anaphase transition for different U2OS cells. Data were collected in 2 independent experiments, total number of analyzed cells n = 67 (control), n = 76 (UBE2S knockdown), n = 67 (CDC20 knockdown) and n = 62 (UBE2S and CDC20 knockdown). Median, 25% and 75%

percentiles are shown. ** indicates p<0.001, **** indicates p<0.0001 as calculated with Kruskal Wallis test followed by Dunn's multiple comparison test. Right panel, western blot showing successful knockdown of UBE2S and CDC20 in U2OS H2B-mCherry. **d**, Western blot in (**3g**) with the addition of levels of endogenous or recombinant variants of UBE2S. Uncropped images for panels (**a,d**) and data for the graph in (**c**) are available as source data.

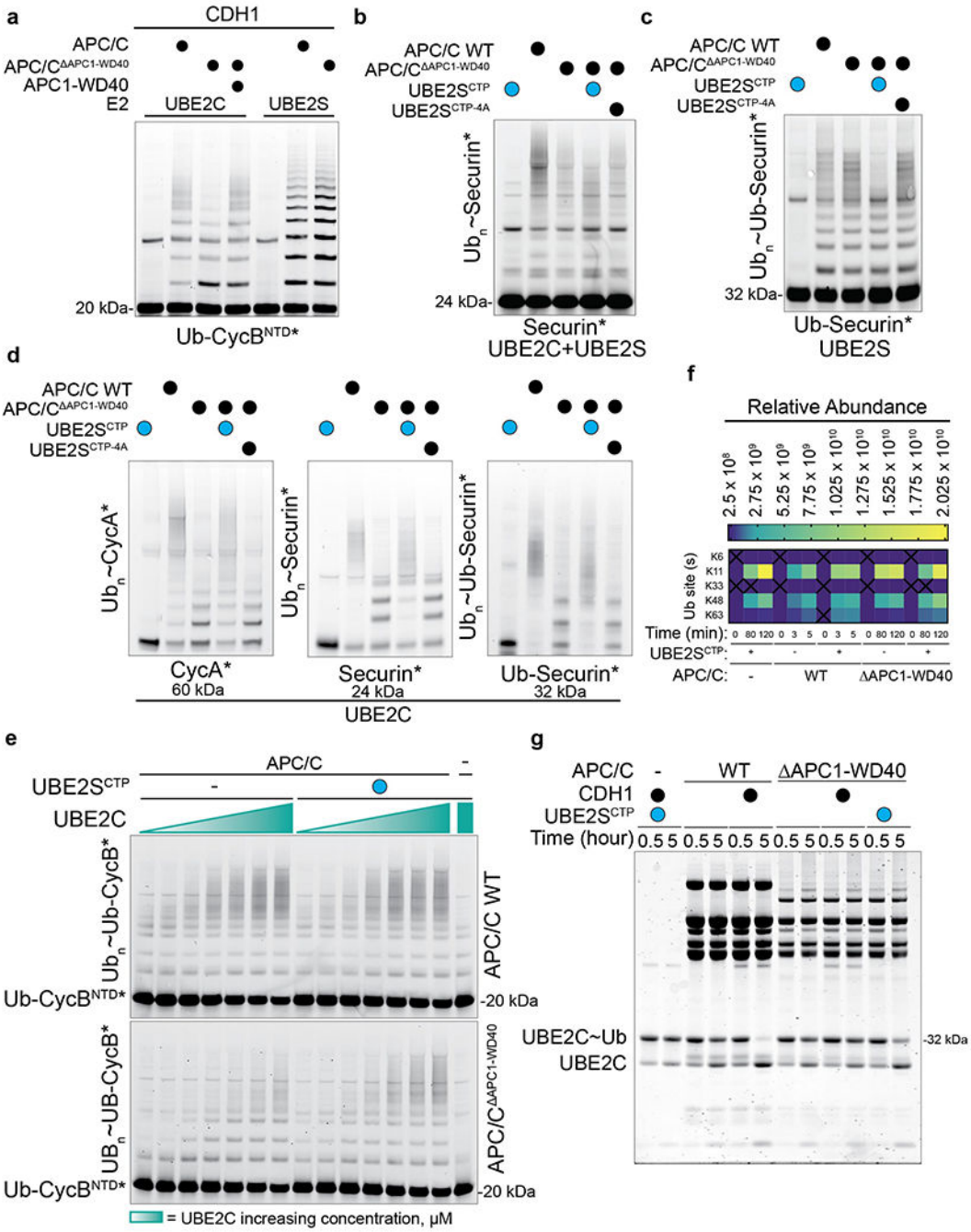

Extended Data Fig. 6. UBE2S^{CTP} activates an otherwise inactive APC/C variant (APC/C$^{\Delta APC1\text{-}WD40}$).

a, As previously reported, APC/C$^{\Delta APC1\text{-}WD40}$ is defective for UBE2C-dependent polyubiquitination, but rescued by the addition of the purified APC1-WD40 domain added *in* trans, monitored by SDS-PAGE and fluorescent scanning[12]. **b**, Assays as in (**4b**), showing the effects of the UBE2S^{CTP} on the polyubiquitination of Securin* by APC/C^{CDH1} (wild-type and indicated variant), UBE2C, and UBE2S. **c**, Assays as in (**4c**), showing the effects of the UBE2S^{CTP} on Ub chain elongation of Ub-Securin by APC/C^{CDH1} (wild-type and

indicated variant) and UBE2S. d, Assays as in (**4d-e**), showing the effects of the UBE2S^{CTP} on the polyubiquitination of multiple substrate by APC/C^{CDH1} (wild-type and indicated variant) and UBE2C. **e**, Representative fluorescent scans of full SDS-PAGE gels in (**4f**) for data used to determine kinetic parameters upon titrating UBE2C in assays measuring UBE2C-dependent ubiquitination for Ub-CycB^{NTD*} with APC/C^{CDH1} (wild-type and indicated variant). **f**, Heat map of Ub-linkages from reactions in (**4g**) analyzed by label free mass spectrometry. Average of n=3 independent experiments. **g**, APC/C activation by UBE2S^{CTP} bypasses the requirement for the APC1-WD40 domain. Representative full gel of hydrolysis of UBE2C~Ub monitored by Sypro-stained SDS-PAGE gels (**4h**). Uncropped image for panel (**g**) and data for the graph in (**f**) are available as source data.

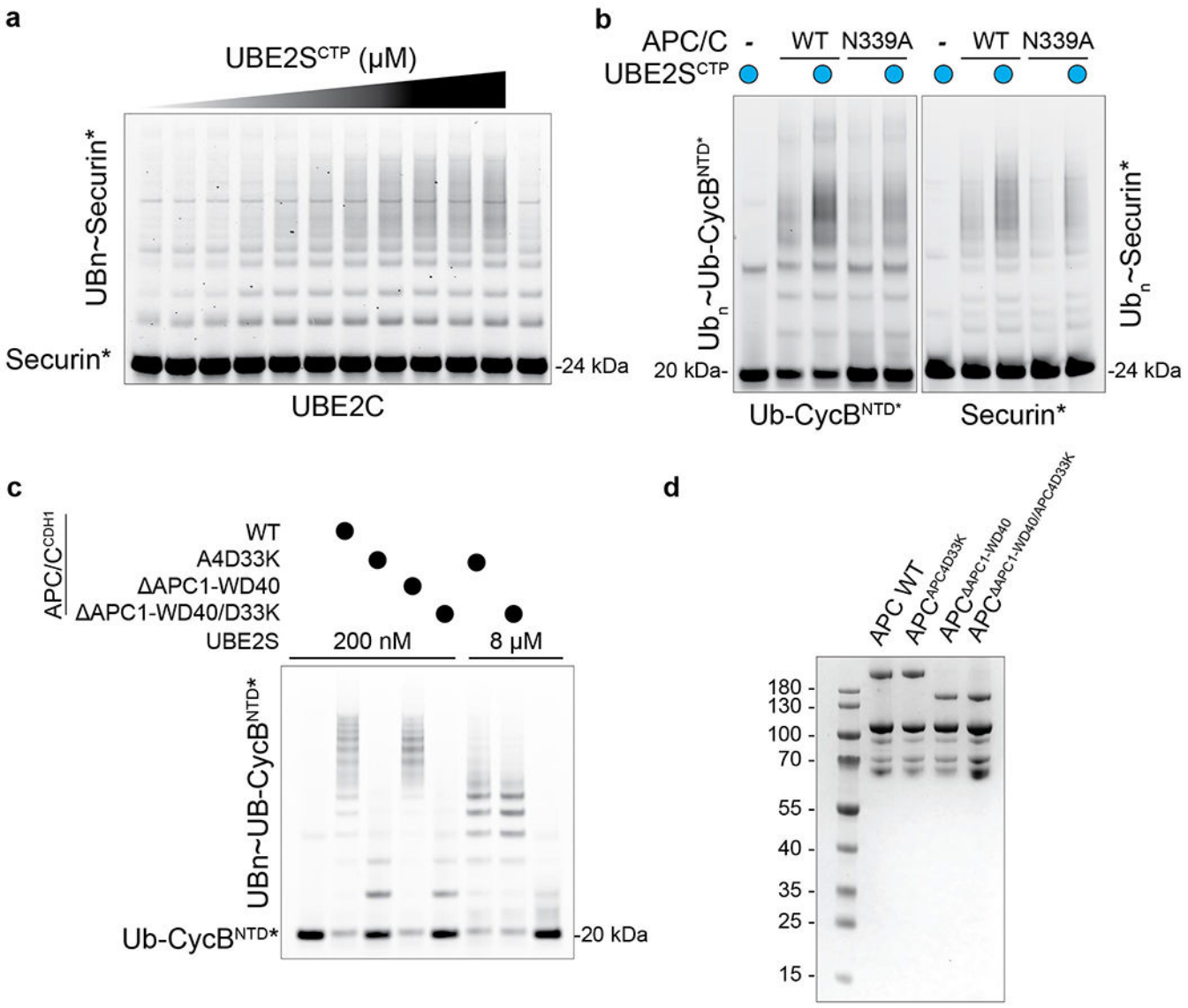

Extended Data Fig. 7. APC/C activation is mediated by UBE2S^{CTP} binding to the APC2–APC4 groove.

a, Representative SDS-PAGE gels in (**5b**) for data used to determine kinetic parameters in titrating the UBE2SCTP in assays measuring Securin* polyubiquitination by APC/C$^{ΔAPC1-WD40}$, CDH1, and UBE2C. **b**, As in assays in (**5e**), UBE2S**CTP** restores UBE2C-dependent substrate polyubiquitination in APC/C variant defective in CDH1-dependent activation. **c**, Mutation of the APC2–APC4 groove prevents Ub chain elongation of Ub-CycB^{NTD*} by APC/C (wild-type and indicated variants) and UBE2S. **d**, Coomassie-stained SDS-PAGE gel of purified wild-type and mutant recombinant APC/Cs. Uncropped image for panel (**b**) is available as source data.

ACKNOWLEDGEMENTS

We thank M. Brunner, R. VanderLinden, and B. Schulman (St. Jude Children's Research Hospital/HHMI/Max Planck Institute of Biochemistry) for providing reagents, E. Salmon (University of North Carolina) for providing

cell lines, and T. Kenakin for helpful discussions. Our work is supported by NIH T32GM008570 and NSF DGE-1650116 (TB and MEG); NIH T32CA009156 (GDG); NIH P30CA016086 (UNC High-throughput peptide Synthesis Facility and Array Facility); NIH R01GM083024, NIH R01GM102413, and the W.M. Keck Foundation (JGC); Hertha Firnberg Program of the Austrian Science Fund (RQ); Boehringer Ingelheim, the Austrian Research Promotion Agency (Headquarter grant FFG-852936), the European Research Council (ERC) under the European Union's Horizon 2020 research and innovation programme GA No 693949, and Human Frontier Science Program grant RGP0057/2018 (J-MP); NIH R01AG011085 (JWH); UNC University Cancer Research Fund (UCRF), NIH R01GM120309, and the American Cancer Society RSG-18-220-01-TBG (MJE); and NIH R35GM128855 and UCRF (NGB).

REFERENCES

1. Metzger MB, Pruneda JN, Klevit RE & Weissman AM RING-type E3 ligases: master manipulators of E2 ubiquitin-conjugating enzymes and ubiquitination. Biochim Biophys Acta 1843, 47–60, doi:10.1016/j.bbamcr.2013.05.026 (2014). [PubMed: 23747565]
2. Streich FC Jr. & Lima CD Structural and functional insights to ubiquitin-like protein conjugation. Annu Rev Biophys 43, 357–379, doi:10.1146/annurev-biophys-051013-022958 (2014). [PubMed: 24773014]
3. Rape M Ubiquitylation at the crossroads of development and disease. Nat Rev Mol Cell Biol 19, 59–70, doi:10.1038/nrm.2017.83 (2018). [PubMed: 28928488]
4. Buetow L & Huang DT Structural insights into the catalysis and regulation of E3 ubiquitin ligases. Nat Rev Mol Cell Biol 17, 626–642, doi:10.1038/nrm.2016.91 (2016). [PubMed: 27485899]
5. King RW, Deshaies RJ, Peters JM & Kirschner MW How proteolysis drives the cell cycle. Science 274, 1652–1659, doi:10.1126/science.274.5293.1652 (1996). [PubMed: 8939846]
6. Peters JM SCF and APC: the Yin and Yang of cell cycle regulated proteolysis. Curr Opin Cell Biol 10, 759–768 (1998). [PubMed: 9914180]
7. Rodrigo-Brenni MC & Morgan DO Sequential E2s drive polyubiquitin chain assembly on APC targets. Cell 130, 127–139, doi:10.1016/j.cell.2007.05.027 (2007). [PubMed: 17632060]
8. Wu K, Kovacev J & Pan ZQ Priming and extending: a UbcH5/Cdc34 E2 handoff mechanism for polyubiquitination on a SCF substrate. Mol Cell 37, 784–796, doi:10.1016/j.molcel.2010.02.025 (2010). [PubMed: 20347421]
9. Haakonsen DL & Rape M Branching Out: Improved Signaling by Heterotypic Ubiquitin Chains. Trends Cell Biol 29, 704–716, doi:10.1016/j.tcb.2019.06.003 (2019). [PubMed: 31300189]
10. Wieser S & Pines J The biochemistry of mitosis. Cold Spring Harb Perspect Biol 7, a015776, doi:10.1101/cshperspect.a015776 (2015). [PubMed: 25663668]
11. Kernan J, Bonacci T & Emanuele MJ Who guards the guardian? Mechanisms that restrain APC/C during the cell cycle. Biochim Biophys Acta Mol Cell Res 1865, 1924–1933, doi:10.1016/j.bbamcr.2018.09.011 (2018). [PubMed: 30290241]
12. Huang J & Bonni A A decade of the anaphase-promoting complex in the nervous system. Genes Dev 30, 622–638, doi:10.1101/gad.274324.115 (2016). [PubMed: 26980187]
13. Alfieri C, Zhang S & Barford D Visualizing the complex functions and mechanisms of the anaphase promoting complex/cyclosome (APC/C). Open Biol 7, doi:10.1098/rsob.170204 (2017).
14. Watson ER, Brown NG, Peters JM, Stark H & Schulman BA Posing the APC/C E3 Ubiquitin Ligase to Orchestrate Cell Division. Trends Cell Biol 29, 117–134, doi:10.1016/j.tcb.2018.09.007 (2019). [PubMed: 30482618]
15. Visintin R, Prinz S & Amon A CDC20 and CDH1: a family of substrate-specific activators of APC-dependent proteolysis. Science 278, 460–463, doi:10.1126/science.278.5337.460 (1997). [PubMed: 9334304]
16. Kim S & Yu H Mutual regulation between the spindle checkpoint and APC/C. Semin Cell Dev Biol 22, 551–558, doi:10.1016/j.semcdb.2011.03.008 (2011). [PubMed: 21439394]
17. Musacchio A The Molecular Biology of Spindle Assembly Checkpoint Signaling Dynamics. Curr Biol 25, R1002–1018, doi:10.1016/j.cub.2015.08.051 (2015). [PubMed: 26485365]
18. Reimann JD, Gardner BE, Margottin-Goguet F & Jackson PK Emi1 regulates the anaphase-promoting complex by a different mechanism than Mad2 proteins. Genes Dev 15, 3278–3285, doi:10.1101/gad.945701 (2001). [PubMed: 11751633]

19. Chang LF, Zhang Z, Yang J, McLaughlin SH & Barford D Molecular architecture and mechanism of the anaphase-promoting complex. Nature 513, 388–393, doi:10.1038/nature13543 (2014). [PubMed: 25043029]
20. da Fonseca PC et al. Structures of APC/C(Cdh1) with substrates identify Cdh1 and Apc10 as the D-box co-receptor. Nature 470, 274–278, doi:10.1038/nature09625 (2011). [PubMed: 21107322]
21. Buschhorn BA et al. Substrate binding on the APC/C occurs between the coactivator Cdh1 and the processivity factor Doc1. Nat Struct Mol Biol 18, 6–13, doi:10.1038/nsmb.1979 (2011). [PubMed: 21186364]
22. Kraft C, Vodermaier HC, Maurer-Stroh S, Eisenhaber F & Peters JM The WD40 propeller domain of Cdh1 functions as a destruction box receptor for APC/C substrates. Mol Cell 18, 543–553, doi:10.1016/j.molcel.2005.04.023 (2005). [PubMed: 15916961]
23. Kimata Y, Baxter JE, Fry AM & Yamano H A role for the Fizzy/Cdc20 family of proteins in activation of the APC/C distinct from substrate recruitment. Mol Cell 32, 576–583, doi:10.1016/j.molcel.2008.09.023 (2008). [PubMed: 19026787]
24. Chang L, Zhang Z, Yang J, McLaughlin SH & Barford D Atomic structure of the APC/C and its mechanism of protein ubiquitination. Nature 522, 450–454, doi:10.1038/nature14471 (2015). [PubMed: 26083744]
25. Brown NG et al. RING E3 mechanism for ubiquitin ligation to a disordered substrate visualized for human anaphase-promoting complex. Proc Natl Acad Sci U S A 112, 5272–5279, doi:10.1073/pnas.1504161112 (2015). [PubMed: 25825779]
26. Li Q et al. WD40 domain of Apc1 is critical for the coactivator-induced allosteric transition that stimulates APC/C catalytic activity. Proc Natl Acad Sci U S A 113, 10547–10552, doi:10.1073/pnas.1607147113 (2016). [PubMed: 27601667]
27. Brown NG et al. Dual RING E3 Architectures Regulate Multiubiquitination and Ubiquitin Chain Elongation by APC/C. Cell 165, 1440–1453, doi:10.1016/j.cell.2016.05.037 (2016). [PubMed: 27259151]
28. Aristarkhov A et al. E2-C, a cyclin-selective ubiquitin carrier protein required for the destruction of mitotic cyclins. Proc Natl Acad Sci U S A 93, 4294–4299, doi:10.1073/pnas.93.9.4294 (1996). [PubMed: 8633058]
29. Yu H, King RW, Peters JM & Kirschner MW Identification of a novel ubiquitin-conjugating enzyme involved in mitotic cyclin degradation. Curr Biol 6, 455–466 (1996). [PubMed: 8723350]
30. Kirkpatrick DS et al. Quantitative analysis of in vitro ubiquitinated cyclin B1 reveals complex chain topology. Nat Cell Biol 8, 700–710, doi:10.1038/ncb1436 (2006). [PubMed: 16799550]
31. Garnett MJ et al. UBE2S elongates ubiquitin chains on APC/C substrates to promote mitotic exit. Nat Cell Biol 11, 1363–1369, doi:10.1038/ncb1983 (2009). [PubMed: 19820702]
32. Wu T et al. UBE2S drives elongation of K11-linked ubiquitin chains by the anaphase-promoting complex. Proc Natl Acad Sci U S A 107, 1355–1360, doi:10.1073/pnas.0912802107 (2010). [PubMed: 20080579]
33. Williamson A et al. Identification of a physiological E2 module for the human anaphase-promoting complex. Proc Natl Acad Sci U S A 106, 18213–18218, doi:10.1073/pnas.0907887106 (2009). [PubMed: 19822757]
34. Lu Y, Wang W & Kirschner MW Specificity of the anaphase-promoting complex: a single-molecule study. Science 348, 1248737, doi:10.1126/science.1248737 (2015). [PubMed: 25859049]
35. Kelly A, Wickliffe KE, Song L, Fedrigo I & Rape M Ubiquitin chain elongation requires E3-dependent tracking of the emerging conjugate. Mol Cell 56, 232–245, doi:10.1016/j.molcel.2014.09.010 (2014). [PubMed: 25306918]
36. Wickliffe KE, Lorenz S, Wemmer DE, Kuriyan J & Rape M The mechanism of linkage-specific ubiquitin chain elongation by a single-subunit E2. Cell 144, 769–781, doi:10.1016/j.cell.2011.01.035 (2011). [PubMed: 21376237]
37. Brown NG et al. Mechanism of polyubiquitination by human anaphase-promoting complex: RING repurposing for ubiquitin chain assembly. Mol Cell 56, 246–260, doi:10.1016/j.molcel.2014.09.009 (2014). [PubMed: 25306923]

38. Frye JJ et al. Electron microscopy structure of human APC/C(CDH1)-EMI1 reveals multimodal mechanism of E3 ligase shutdown. Nat Struct Mol Biol 20, 827–835, doi:10.1038/nsmb.2593 (2013). [PubMed: 23708605]
39. Meyer HJ & Rape M Enhanced protein degradation by branched ubiquitin chains. Cell 157, 910–921, doi:10.1016/j.cell.2014.03.037 (2014). [PubMed: 24813613]
40. Qiao R et al. Mechanism of APC/CCDC20 activation by mitotic phosphorylation. Proc Natl Acad Sci U S A 113, E2570–2578, doi:10.1073/pnas.1604929113 (2016). [PubMed: 27114510]
41. Van Voorhis VA & Morgan DO Activation of the APC/C ubiquitin ligase by enhanced E2 efficiency. Curr Biol 24, 1556–1562, doi:10.1016/j.cub.2014.05.052 (2014). [PubMed: 24930963]
42. Sako K et al. Emi2 mediates meiotic MII arrest by competitively inhibiting the binding of Ube2S to the APC/C. Nat Commun 5, 3667, doi:10.1038/ncomms4667 (2014). [PubMed: 24770399]
43. Matyskiela ME & Morgan DO Analysis of activator-binding sites on the APC/C supports a cooperative substrate-binding mechanism. Mol Cell 34, 68–80, doi:10.1016/j.molcel.2009.02.027 (2009). [PubMed: 19362536]
44. Craney A et al. Control of APC/C-dependent ubiquitin chain elongation by reversible phosphorylation. Proc Natl Acad Sci U S A 113, 1540–1545, doi:10.1073/pnas.1522423113 (2016). [PubMed: 26811472]
45. Yamaguchi M et al. Cryo-EM of Mitotic Checkpoint Complex-Bound APC/C Reveals Reciprocal and Conformational Regulation of Ubiquitin Ligation. Mol Cell 63, 593–607, doi:10.1016/j.molcel.2016.07.003 (2016). [PubMed: 27522463]
46. Alfieri C et al. Molecular basis of APC/C regulation by the spindle assembly checkpoint. Nature 536, 431–436, doi:10.1038/nature19083 (2016). [PubMed: 27509861]
47. Rodriguez C et al. A novel human Cdh1 mutation impairs anaphase promoting complex/cyclosome activity resulting in microcephaly, psychomotor retardation, and epilepsy. J Neurochem, doi:10.1111/jnc.14828 (2019).
48. Paiva SL & Crews CM Targeted protein degradation: elements of PROTAC design. Curr Opin Chem Biol 50, 111–119, doi:10.1016/j.cbpa.2019.02.022 (2019). [PubMed: 31004963]
49. Fujimitsu K, Grimaldi M & Yamano H Cyclin-dependent kinase 1-dependent activation of APC/C ubiquitin ligase. Science 352, 1121–1124, doi:10.1126/science.aad3925 (2016). [PubMed: 27103671]
50. Zhang S et al. Molecular mechanism of APC/C activation by mitotic phosphorylation. Nature 533, 260–264, doi:10.1038/nature17973 (2016). [PubMed: 27120157]
51. Baek K et al. NEDD8 nucleates a multivalent cullin-RING-UBE2D ubiquitin ligation assembly. Nature 578, 461–466, doi:10.1038/s41586-020-2000-y (2020). [PubMed: 32051583]
52. Kelsall IR et al. TRIAD1 and HHARI bind to and are activated by distinct neddylated Cullin-RING ligase complexes. EMBO J 32, 2848–2860, doi:10.1038/emboj.2013.209 (2013). [PubMed: 24076655]
53. Scott DC et al. Two Distinct Types of E3 Ligases Work in Unison to Regulate Substrate Ubiquitylation. Cell 166, 1198–1214 e1124, doi:10.1016/j.cell.2016.07.027 (2016). [PubMed: 27565346]
54. Dueber EC et al. Antagonists induce a conformational change in cIAP1 that promotes autoubiquitination. Science 334, 376–380, doi:10.1126/science.1207862 (2011). [PubMed: 22021857]
55. Feltham R et al. Smac mimetics activate the E3 ligase activity of cIAP1 protein by promoting RING domain dimerization. J Biol Chem 286, 17015–17028, doi:10.1074/jbc.M111.222919 (2011). [PubMed: 21393245]
56. Stewart MD, Ritterhoff T, Klevit RE & Brzovic PS E2 enzymes: more than just middle men. Cell Res 26, 423–440, doi:10.1038/cr.2016.35 (2016). [PubMed: 27002219]
57. Pierce NW, Kleiger G, Shan SO & Deshaies RJ Detection of sequential polyubiquitylation on a millisecond timescale. Nature 462, 615–619, doi:10.1038/nature08595 (2009). [PubMed: 19956254]
58. Kleiger G, Saha A, Lewis S, Kuhlman B & Deshaies RJ Rapid E2-E3 assembly and disassembly enable processive ubiquitylation of cullin-RING ubiquitin ligase substrates. Cell 139, 957–968, doi:10.1016/j.cell.2009.10.030 (2009). [PubMed: 19945379]

59. Koegl M et al. A novel ubiquitination factor, E4, is involved in multiubiquitin chain assembly. Cell 96, 635–644, doi:10.1016/s0092-8674(00)80574-7 (1999). [PubMed: 10089879]

60. Jarvis MA et al. Measuring APC/C-Dependent Ubiquitylation In Vitro. Methods Mol Biol 1342, 287–303, doi:10.1007/978-1-4939-2957-3_18 (2016). [PubMed: 26254932]

61. Yamaguchi M et al. Structure of an APC3-APC16 complex: insights into assembly of the anaphase-promoting complex/cyclosome. J Mol Biol 427, 1748–1764, doi:10.1016/j.jmb.2014.11.020 (2015). [PubMed: 25490258]

62. Pickart CM & Raasi S Controlled synthesis of polyubiquitin chains. Methods Enzymol 399, 21–36, doi:10.1016/S0076-6879(05)99002-2 (2005). [PubMed: 16338346]

63. White HD & Rayment I Kinetic characterization of reductively methylated myosin subfragment 1. Biochemistry 32, 9859–9865, doi:10.1021/bi00088a042 (1993). [PubMed: 8373784]

64. Bonacci T et al. Cezanne/OTUD7B is a cell cycle-regulated deubiquitinase that antagonizes the degradation of APC/C substrates. EMBO J 37, doi:10.15252/embj.201798701 (2018).

65. Williamson A, Jin L & Rape M Preparation of synchronized human cell extracts to study ubiquitination and degradation. Methods Mol Biol 545, 301–312, doi:10.1007/978-1-60327-993-2_19 (2009). [PubMed: 19475397]

66. Moggridge S, Sorensen PH, Morin GB & Hughes CS Extending the Compatibility of the SP3 Paramagnetic Bead Processing Approach for Proteomics. J Proteome Res 17, 1730–1740, doi:10.1021/acs.jproteome.7b00913 (2018). [PubMed: 29565595]

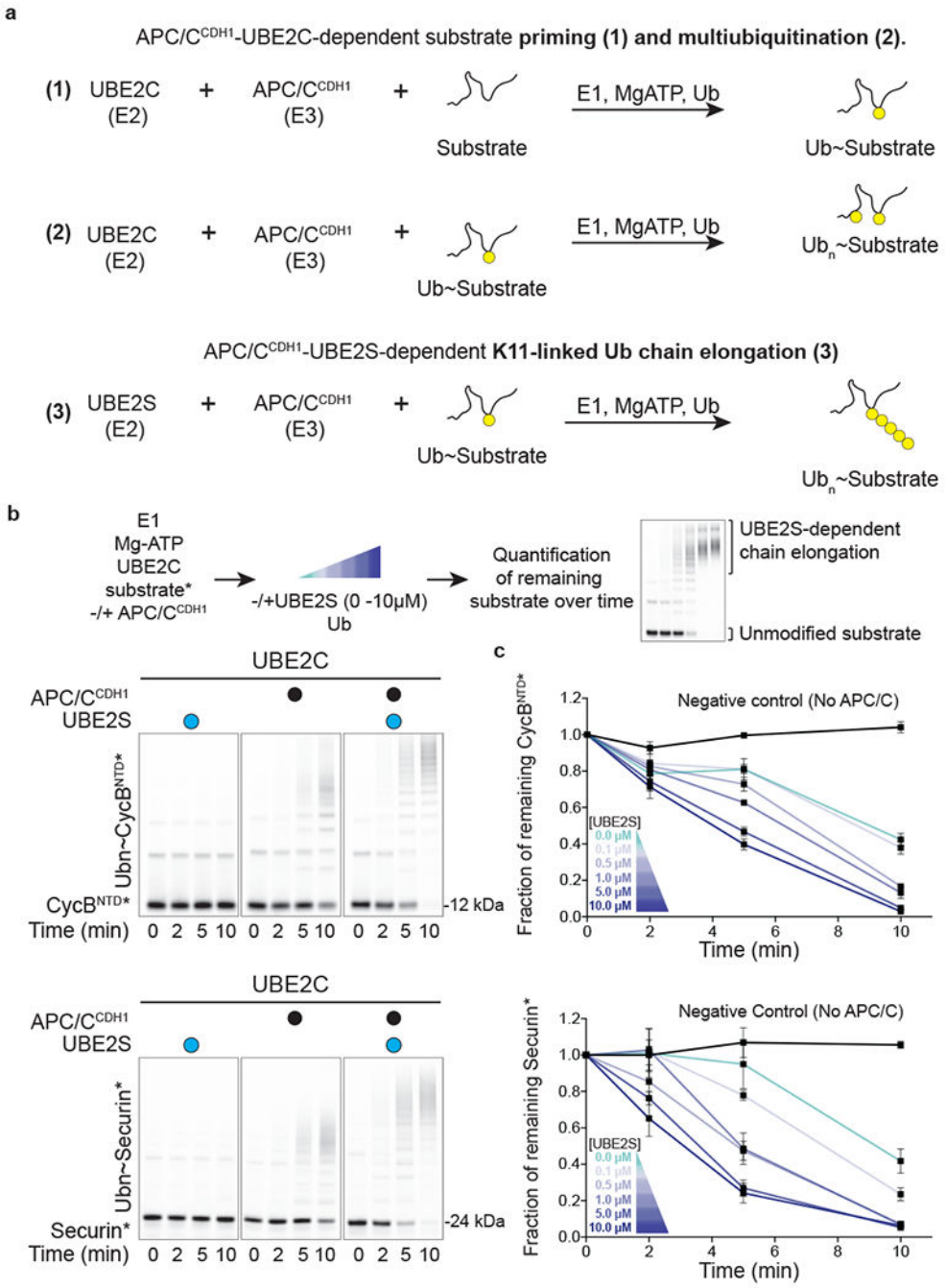

Figure 1. UBE2S increases the rate of substrate modification by APC/C^{CDH1}-UBE2C.

a, Outline of APC/C-mediated substrate priming by UBE2C, multiubiquitination by UBE2C, and K11-linked Ub chain elongation by UBE2S. **b**, Addition of UBE2S to APC/C^{CDH1}-dependent substrate (CycB^{NTD}*, Top, and Securin*, Bottom) polyubiquitination reactions containing UBE2C accelerates substrate consumption. Substrates are fluorescently labeled and modifications are resolved by SDS-PAGE and fluorescence scanning. Representative fluorescent scans of APC/C-dependent ubiquitination reactions. Negative control reactions do not contain APC/C. **c**, Quantitation of ubiquitination reactions shown in

(b) depicted as fraction of substrate remaining over time. UBE2S increases the fraction of substrate modified over time in a dose-dependent manner as shown for $CycB^{NTD*}$ (Top) and Securin (Bottom). Average of n=3 independent experiments ± s.e.m. Uncropped images for panel **(b)** and data for graphs in **(c)** are available as source data.

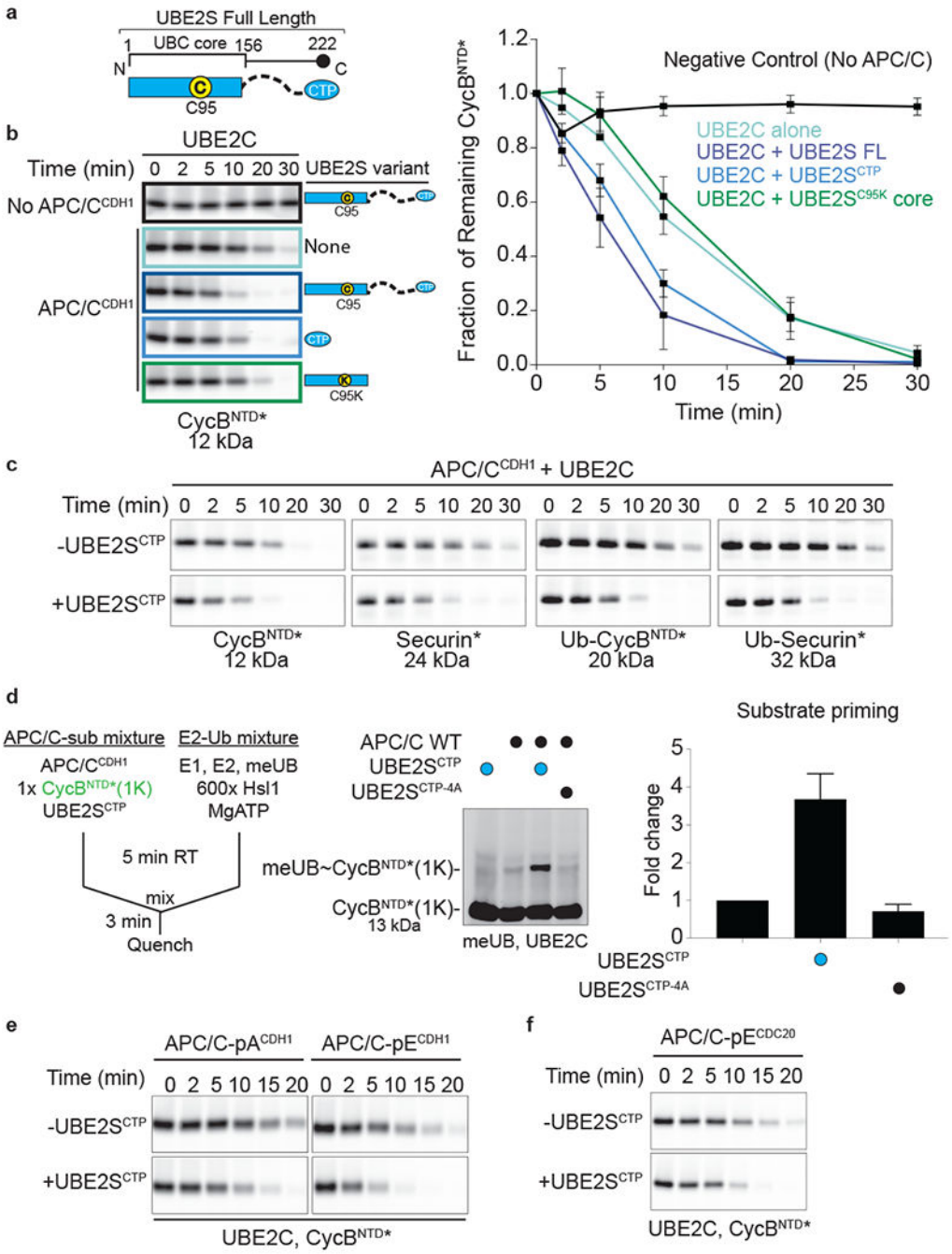

Figure 2. UBE2S^{CTP} is responsible for rate enhancement of substrate priming and multiubiquitination by APC/C-UBE2C.

a, Schematic diagram of the domain architecture of UBE2S. The catalytic core is conserved among E2s (UBC core, residues 1-156), the C-terminal extension includes a linker (residues 157-203) from which the C-terminal peptide extends (CTP, residues 204-222). **b**, Similar to 1b, time courses of APC/C^{CDH1}-UBE2C-dependent reactions in the presence or absence of full-length UBE2S or UBE2S domains (Left) show that UBE2S^{CTP} increases the rate of CycB^{NTD}* depletion similar to full-length UBE2S, quantification depicts relative fraction of

remaining unmodified CycB^{NTD}*. Average of n=3 independent experiments ± s.e.m. (Right). **c**, Ubiquitination assays similar to **(b)** showing unmodified substrate levels over time and comparing the effect of UBE2S^{CTP} on multiple substrates. UBE2S^{CTP} accelerates APC/C^{CDH1}-UBE2C-dependent modification for all substrates tested. **d**, Schematic of experimental setup of single encounter assay (Left). In brief, APC/C^{CDH1}, fluorescent substrate, and UBE2S^{CTP} are pre-incubated in one reaction mix; E1, UBE2C, methylated ubiquitin (meUb), ATP, and an excess of unlabeled substrate are combined in a second mix. Combining the mixtures initiates substrate ubiquitination during a single substrate-binding event (Middle). Quantification and normalization of primed CycB^{NTD}*(1K) represented as fold change relative to reactions without the UBE2S^{CTP} (Right). A variant peptide where residues 219-222 where substituted to alanine (UBE2S^{CTP-4A}) was used as a negative control. Average of n=3 independent experiments ± s.e.m. (Right). **e-f**, Assays as in **(c)** testing versions of the APC/C that mimic its different states during the cell cycle. UBE2S^{CTP} is supplemented in UBE2C-dependent reactions. Levels of unmodified CycB^{NTD}* are followed over time using different APC/C variants, APC/C-pA and APC/C-pE **(e)** and coactivators, CDH1 and CDC20 **(e-f)**. Uncropped images for panels **(b-f)** and data for graphs in **(b,d)** are available as source data.

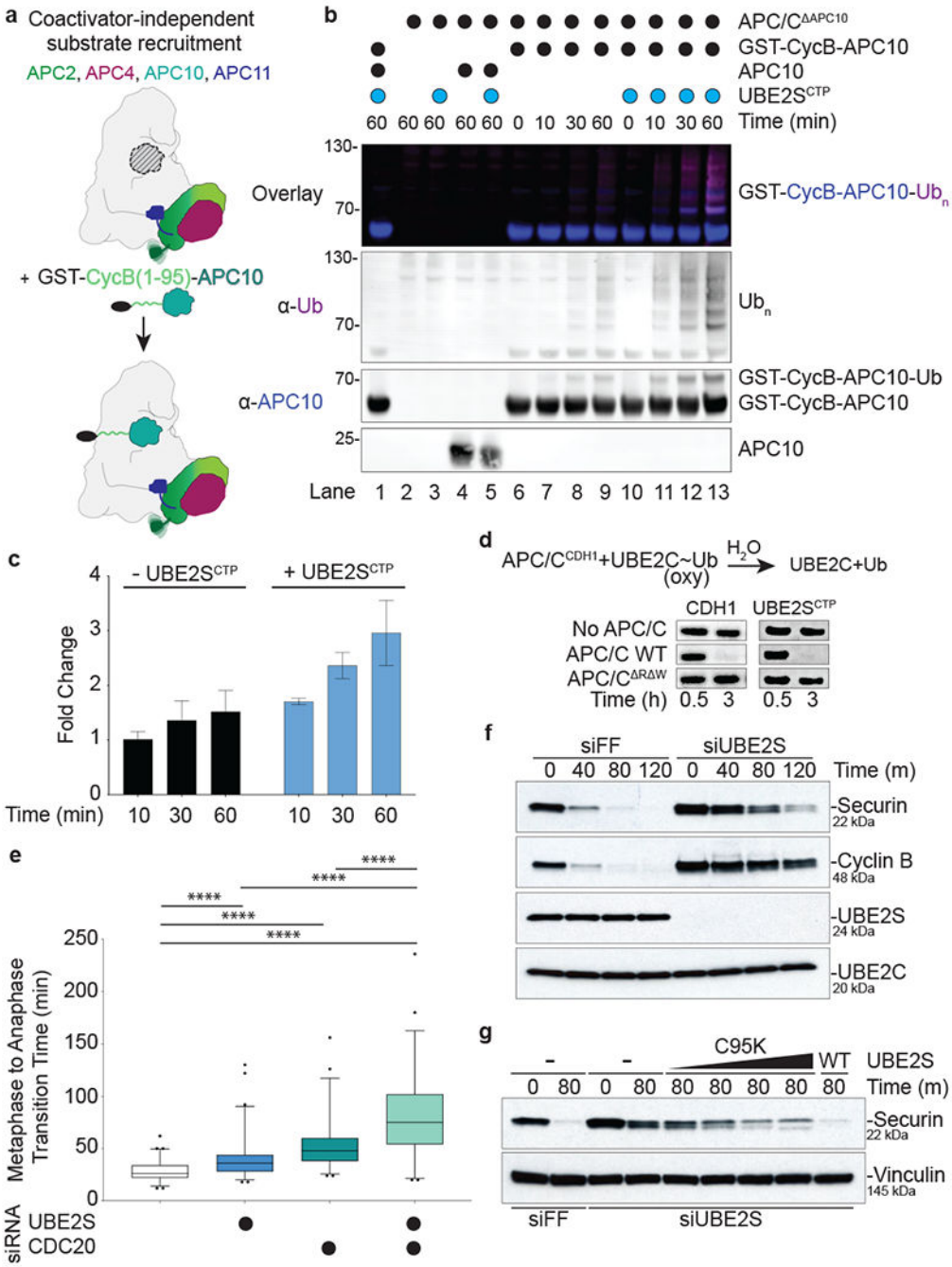

Figure 3. UBE2S^{CTP} stimulates APC/C in a coactivator independent manner.

a, Schematic showing UBE2C-dependent ubiquitination reaction bypasses coactivator-dependent substrate recruitment by adding a substrate (CycB^{NTD})-fused APC10 to APC/C lacking APC10 (APC/C$^{\Delta APC10}$). **b**, Effect of UBE2S^{CTP} on APC/C activation in a coactivator-independent manner probed by monitoring APC10-CycB and Ub via western blot using antibodies against APC10 (blue) and Ub (red). **c**, Bar graph quantifying ubiquitination levels in assays shown in **(b)**, showing increased levels of ubiquitination upon the addition of UBE2S^{CTP}. Fold change is relative to 0 min. Average of n=3 independent

experiments ± s.e.m. **d**, CDH1 and UBE2S^{CTP} stimulate the APC/C to promote UBE2C~Ub activation in an APC11^{RING}(R)- and APC2^{WHB}(W)-dependent manner. Coomassie-stained SDS-PAGE gel images depict the hydrolysis of UBE2C~Ub. **e**, Time necessary for the metaphase to anaphase transition. Data were collected in 3 independent experiments, total number of analyzed cells n=126 (control), n=125 (knockdown of UBE2S), n=118 (knockdown of CDC20) and n=128 (knockdown of UBE2S and CDC20). A total of n=4 (control) and n=20 (UBE2S and CDC20 knockdown) cells did not successfully segregate chromosomes and were not included in defining the boxplots. Median, 25% and 75% percentiles are shown. **** indicates $p<0.0001$ as calculated with Kruskal Wallis test followed by Dunn's multiple comparison test. **f**, G1 extracts were prepared from HeLa S3 cells transfected with either control or UBE2S siRNA. Cyclin B and Securin degradation, monitored by immunoblot, is significantly impaired in UBE2S-depleted extracts. **g**, UBE2S-depleted G1 extracts, as in **(f)**, were supplemented with increasing concentrations of recombinant UBE2S^{C95K} (1.25 μM, 2.5 μM, 5 μM,10 μM) or 1 μM recombinant UBE2S WT. Reactions were collected at indicated time points and Securin degradation was analyzed by immunoblot. Uncropped images for panels (**b, d, f-g**) and data for graphs in (**c, e**) are available as source data.

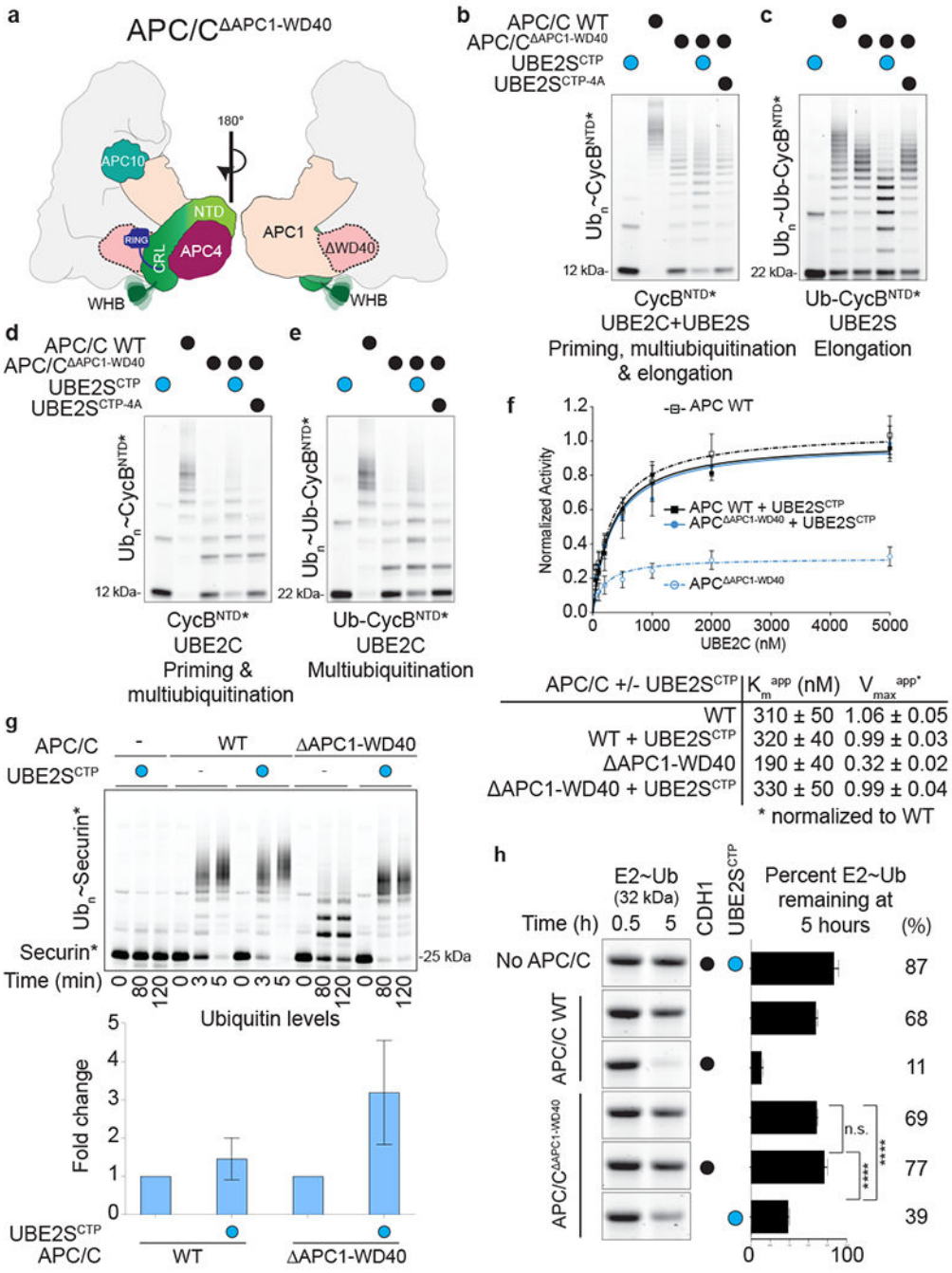

Figure 4. UBE2S^{CTP} restores the activity of an APC/C variant defective in coactivator-dependent activation.

a, Cartoon representing APC/C$^{\Delta APC1\text{-}WD40}$ showing the catalytic core locked in a downward position and inaccessible for UBE2C recruitment, based on previous studies[26]. **b**, Substrate ubiquitination reactions comparing the effects of UBE2S^{CTP} and UBES^{CTP-4A} (residues 219-222 of UBE2S^{CTP} substituted for alanine) on CycB^{NTD}* priming, multiubiquitination, and Ub chain elongation by APC/C$^{\Delta APC1\text{-}WD40}$, UBE2C, and UBE2S. **c**, Testing the effects of UBE2S^{CTP} on Ub chain elongation by APC/C$^{\Delta APC1\text{-}WD40}$ and UBE2S. **d**, Testing the

effects of UBE2S^{CTP} on priming and multiubiquitination by APC/C$^{\Delta APC1\text{-}WD40}$ and UBE2C. **e**, Testing the effects of UBE2S^{CTP} on UBE2C-dependent multiubiquitination by APC/C$^{\Delta APC1\text{-}WD40}$ and UBE2C. **f**, Titration of UBE2C in ubiquitination reactions using APC/C and APC/C$^{\Delta APC1\text{-}WD40}$. Addition of UBE2S^{CTP} rescues defective APC/C$^{\Delta APC1\text{-}WD40}$-dependent ubiquitination. Kinetic parameters measured by quantifying levels of modified substrate and plotted using the Michaelis-Menton equation to show that the addition of UBE2S^{CTP} restores APC/C$^{\Delta APC1\text{-}WD40}$ to WT levels. Average of n=6 independent experiments ± s.e.m. **g**, UBE2S^{CTP} increases levels of ubiquitination of Securin* by APC/C$^{\Delta APC1\text{-}WD40}$ and UBE2C. Representative fluorescent scans of time courses following Securin* polyubiquitination by APC/C^{CDH1} wild-type and APC/C$^{\Delta APC1\text{-}WD40}$ with UBE2C in the presence and absence of UBE2S^{CTP}. Bar graphs of semi-quantitative mass spectrometry analysis: Fold change in ubiquitination in WT and APC/C$^{\Delta APC1\text{-}WD40}$ at 5 min and 120 min, respectively. Average of n=3 independent experiments ± s.e.m. **h**, Similar to **(3d),** UBE2C~Ub hydrolysis assays showing that APC/C activation by UBE2S^{CTP} bypasses the requirement for the APC1-WD40 domain. Sypro-stained SDS-PAGE gel images depict depletion of unhydrolyzed UBE2C~Ub in an APC/C-dependent manner. Average of n=3 independent experiments ± s.e.m. **** indicates $p<0.0001$ as calculated with ANOVA followed by Tukey's multiple comparison test, ns, not significant. Uncropped images for panels **(b-e, g-h)** and data for graphs in **(f-h)** are available as source data.

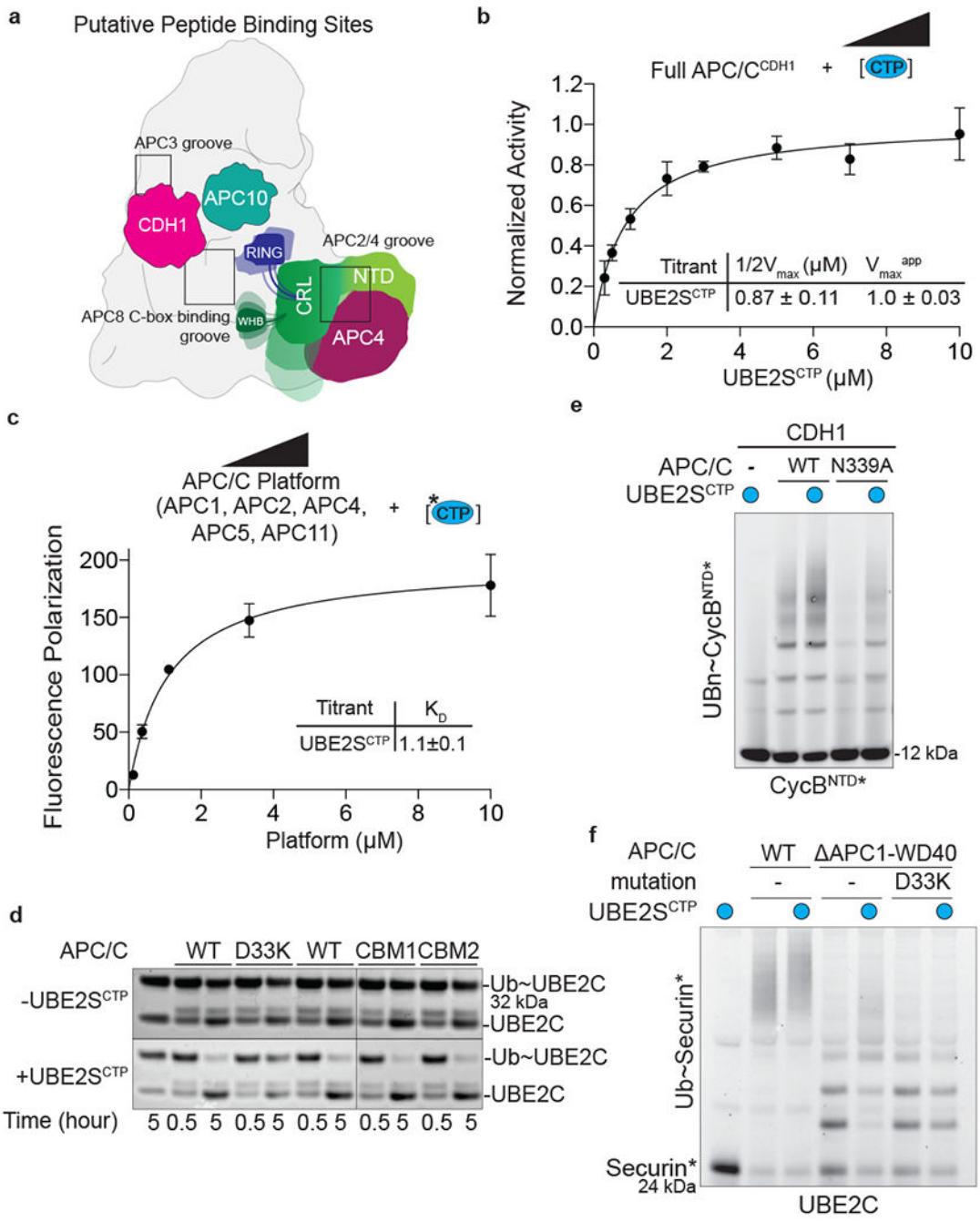

Figure 5. UBE2S CTP binding to APC2–APC4 groove is responsible for APC/C activation.

a, Schematic of APC/C-peptide interactions, APC3 and APC8 bound to the IR and C box of the coactivators, respectively, and the UBE2S^{CTP} bound to the APC2–APC4 groove. **b**, Kinetic parameters of activation of APC/C$^{\Delta APC1WD40}$ determined by titration of UBE2S^{CTP} and monitoring of UBE2C-dependent formation of Ub^{n}~Securin*. Average of n=4 independent experiments ± s.e.m. **c**, UBE2S^{CTP} interacts with the APC/C Platform as shown by changes in fluorescence polarization of fluorescein labeled UBE2S^{CTP} (indicated by *) upon binding to increasing concentrations of the APC/C Platform. Average of n=6

independent experiments ± s.e.m. **d**, UBE2C~Ub hydrolysis reactions using APC/C carrying specific mutations on APC8 (CBM1: N339A:E374R, CBM2: N339A:E410R) or APC2–APC4 (APC4 D33K) to map the binding site of the $UBE2S^{CTP}$. **e**, APC^{CDH1}-UBE2C-dependent substrate ubiquitination reactions showing that $UBE2S^{CTP}$ can restore ubiquitination activity in an APC/C mutant defective for coactivator-dependent activation. **f**, Similar to **(e),** charge-swap mutation at the APC2–APC4 groove prevents the restoration of UBE2C-dependent polyubiquitination of Securin by $APC/C^{\Delta APC1WD40}$. Uncropped images for panels **(d-f)** and data for graphs in **(b-c)** are available as source data.

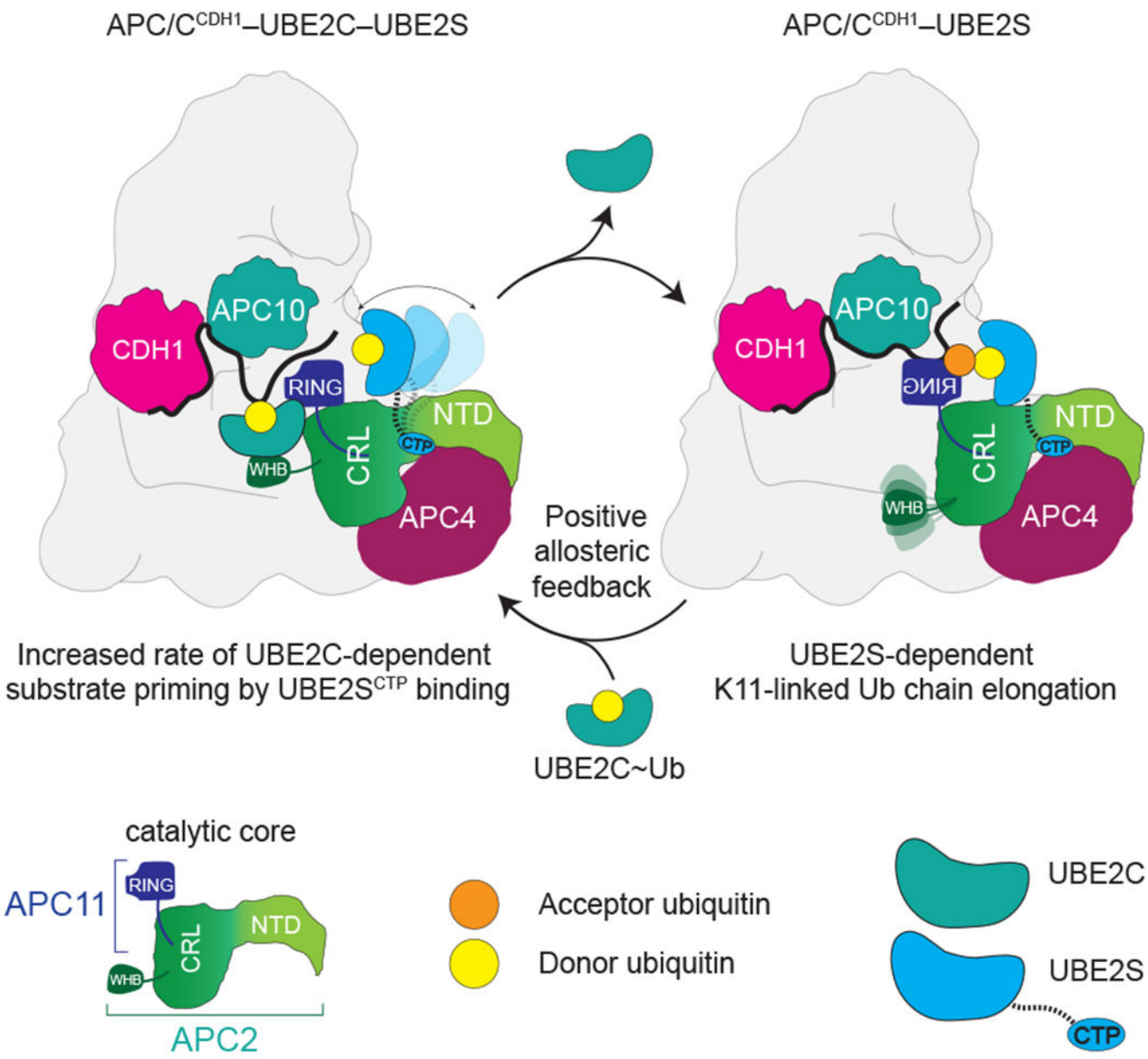

Figure 6. Ub Chain Elongating E2 UBE2S activates the E3 APC/C to function with its priming E2 UBE2C.

Previous models of APC/C activation have ascribed activation solely to canonical coactivators[13,14]. In contrast, our model suggests that the binding of both the APC/C coactivator and the Ub chain elongating E2 UBE2S activate the APC/C (mobilization of the catalytic core) through different allosteric mechanisms. This positive feedback permits UBE2C~Ub recruitment to APC2^{W} and APC11^{RING} to effectively prime substrates with the initial Ub. The substrate-linked Ub is then bound to the repurposed APC11^{RING} domain for Ub chain elongation by UBE2S. UBE2S bound to APC/C facilitates UBE2C~Ub recruitment for further substrate modification, multiubiquitination. Therefore, UBE2S

enhances substrate modification and elongates Ub chains, promoting protein degradation by the APC/C.